Viral Nanoparticles as Lateral Flow Assay Reporters: Analysis of Capture Kinetics, Stabilization, and Detection In Blood

by
Ahmad A. Nazem

A dissertation submitted to the Department of Biomedical Engineering,
Cullen College of Engineering
in partial fulfillment of the requirements for the degree of

Doctor of Philosophy

in Biomedical Engineering

Chair of Committee: Richard C. Willson

Committee Member: Jakoah Brgoch

Committee Member: Dmitri Litvinov

Committee Member: Chandra Mohan

Committee Member: Sergey Shevkoplyas

University of Houston
December 2019

DEDICATION

I dedicate this dissertation to my father, who passed a little over a year ago and helped me in all things, great and small. There are no words that can express how I feel, and I will always thank Almighty Allah for everything. All of my childhood memories and how you raised me was out of love for Almighty Allah and me. You were still there for me when I was sick, happy, or had a tough decision to make. I truly appreciate how blessed I was to have you as my father who always smiled, went out of his way to help people, and had a heart always filled with love. I love you, Dad, and wish you could be here, but Almighty Allah is the best of planners.

ACKNOWLEDGMENTS

I want to extend my sincere gratitude to my advisor, Dr. Richard Willson, for allowing me to work in his lab, contribute to the present work, and funding my time as a graduate student. Dr. Willson has actively supported my research interests while still encouraging diligence to be the best scientist. I would also like to thank Dr. Katerina Kourentzi, who has provided guidance and mentorship through my time in the Willson lab. Special thanks to Dr. Jakoah Brgoch, Dr. Dmitri Litvinov, Dr. Chandra Mohan, and Dr. Sergey Shevkoplyas for their insight and service on my dissertation committee.

Several people in Dr. Willson's lab at the University of Houston have contributed their knowledge, time, and skill to the development of this work. Thank you to Drs. Binh Vu, Mary Crum, Gavin Garvey, Hui Chen, Heather Goux, Jinsu Kim, Andrew Paterson and to, João Trabuco, Ujwal Patil, Max Smith, Dimple Chavan, Victoria Hlavinka, Kristen Brosamer, Atul Goyal, and Suman Nandy for their helpful advice and friendship. I am grateful to the University of Houston, the Biomedical Engineering Department, and the Chemical and Biomolecular Engineering Department. I am thankful for the courses I took and the professors I learned from in my time as a graduate student. I acknowledge support from NIH (1R01AR072742-01), NSF Biosensing (#1511789 and #1928334), NSF RAPID (#175944), CDC (1U01CK000512-01), and Ladies Leukemia League, Inc for funding the research and my time as a graduate student.

Finally, I would like to thank my family for their guidance, encouragement, and unwavering support. I am grateful for my parents, Abu and Millie Nazem, for providing the best upbringing. I appreciate my mom, Millie Nazem, who has always supported me in my endeavors and is one of the most influential people I know, and still inspires me after my father's sudden passing a little over a year ago. I want to thank my brother and sister-in-law Ziyad Nazem and Nafila Mannan for being my supporters. I would also like to thank all of my dad's family, who encouraged and supported me along with my in-laws. Lastly, I thank my wife, Ayesha Pirbhai, for all of her support and for always helping me to do the best. In the end, all thanks and praise are due to Almighty Allah for everything in the past, present, and future.

ABSTRACT

Key advances in healthcare have arisen from the implementation of point-of-care (POC) testing in lightly-equipped laboratories, in the field, or at home. POC tests are used in the detection of various analytes, biomarkers, and pathogens, and are widely used due to their convenience, low cost, and reliability. One of the best-known POC tests is the lateral flow immuno-chromatographic assay (LFA). When used as an LFA reporter particle, M13 bacteriophages have demonstrated low limits of detection in the laboratory, and their integration into a complete practical assay was investigated in this work. We developed a rapid and very sensitive LFA, and demonstrated its storage stability and use with whole blood.

A second line of investigation concerned measurement of the kinetics of LFA reporter interaction and capture in porous matrices. Such measurements have been difficult, especially on time scales below one second. A rapid-filtration system for short-time-scale measurement of the kinetics of binding in membranes is described. The system is composed of a mechanical syringe pump driving fluid through a membrane resting on a stainless-steel mesh membrane, which is connected to a vacuum pump to remove excess fluid, and computer-controlled solenoids to bring the membrane abruptly into and out of fluidic contact with the syringe at precisely-controlled times. We used this technology to characterize the binding of M13 bacteriophage onto LFA membranes at flow rates from 0.5 to 8 mL/sec over times ranging from 50 - 1000 msec. Under optimized conditions, this approach showed an increase in binding in a flow-rate and time-dependent manner. Potential applications

of rapid-filtration analysis include the study of chromatographic and membrane adsorption, membrane-based assays, and medical diagnostics. The integration of M13 bacteriophage into complete LFAs and understanding their capture mechanism will lead to insights on how to improve the sensitivity and utility of LFAs.

TABLE OF CONTENTS

LIST OF FIGURES

CHAPTER 1: POINT OF CARE (POC) DIAGNOSTICS

Diagnostics play critical roles in health care, such as providing appropriate and timely care to patients and data for health surveillance. Obtaining timely patient-level data allows for emergency public health interventions and long-term public health strategies. During the 2013-2106 Ebola outbreak, rapid testing was extremely valuable for improving disease management, patient triage, and isolation[1]. Point-of-care (POC) testing allows for patient diagnosis in physician's offices, rural areas, ambulances, the home, the field, or within hospitals. Additionally, diagnostics are rapid and offer a degree of sensitivity and specificity that is crucial for testing in resource-limited settings enabling quick medical decisions, so diseases can be diagnosed at an early stage, leading to improved health outcomes for patients by allowing early treatment. Analytical targets used in diagnostics are proteins, metabolites, dissolved ions and gases, cell types, microbes, and nucleic acids. These targets can be present in a variety of samples, including blood, saliva, urine, feces, etc[2–5]. POC diagnostics may require a sample or with little or no preparation, need only elementary instruction to detect multiple analytes or markers. Result interpretation may be as simple as viewing a colored spot on a paper or polymer background. However, a subset of POC devices have transitioned to hand-held readers such as mobile phones or to benchtop instruments to provide comprehensive results, and if necessary, devices can control and operate the sample-containing platform and execute the analytical process[6]. While POC testing is commonly used in the health sector and for public health interventions, analytical testing also is used in a wide range of fields from agricultural and water

monitoring, drug abuse detection, or areas where diagnostic tools can provide information in a rapid format compared to traditional testing

Historically, all, health care was similar to “point-of-care” in that it was delivered at the patient home through physician’s visits. With technological advancements and new medical discoveries, care shifted to central points, such as hospitals. With a population boom and new hospitals, large centralized laboratories were established, and over time the development of automated systems for the analysis of patient samples led to cost savings and reduced diagnosis times. From these centralized laboratories, a wide variety of medical tests could be performed in large batches and provided the needed quality control and sensitivity for the desired condition. However, these tests took hours or weeks to return results, and some were laborious and required the use of skilled technicians. Point-of-care devices were used on a limited basis in the hospital for rapid analysis in intensive care units. Over time, centralized laboratories became the primary sites of medical testing. Only a few home tests, such as pregnancy and glucose test kits were available to distribute the burden on the healthcare system[7]. With a growing elderly population and increased patient strains on the healthcare system, the emphasis on healthcare is shifting towards prevention and early disease detection[8–10]. POC testing gives immediate results in non-laboratory settings and requires fewer steps, time, and training compared to medical testing in centralized laboratories. It enables staff to make rapid triage and treatment decisions when diagnosing a patient’s condition or monitoring their treatment. Through this, clinicians can focus on what truly matters in providing effective quality patient care.

The benefits of rapid patient testing extend beyond the bedside and allow for improved efficiencies, productivity, simplified processes, and procedures. Additionally, rapid tests comply with regulatory and performance mandates that can reduce the burden on workers in the health care system[11]. Recent advances have greatly expanded the capability of POC testing systems. With technological advancements, devices now can transmit results wirelessly in real-time to the patient's electronic medical record[12]. Additional improvements have led to systems with features designed to assist hospitals in managing their POC testing programs and ensure compliance with changing laboratory regulations[13]. POC testing integration with the health care system will allow for improved patient care and management.

POC Market and Trends

Due to the advantages involved in POC testing, the market is growing to meet the demands of the next century. In 2016, sales of POC testing reached $18.4 billion, an increase of 3.8% from 2014. In 2021 the total global POC diagnostic testing market is expected to reach $23 billion with a growth rate of 4.6% from 2016-2021. Other market studies have predicted faster growth rates in specific countries, with the global POC testing market to grow in the U.S. from $23.2 in 2016 to $40 billion in 2021 at a compound annual growth rate (CAGR) of 10%[14,15]. For the United Kingdom (UK), the expected growth rate is slightly different due to the variety of POC tests being used (Fig. 1). The demands of each healthcare system will vary as specific diseases and conditions are region-specific. Fertility tests, glucose tests, and infectious diseases comprise 45% of the total POC market, while significant parts of the market include

testing for HIV, tuberculosis, hospital-acquired infections, clostridium difficile, and vancomycin-resistant enterococcus[15].

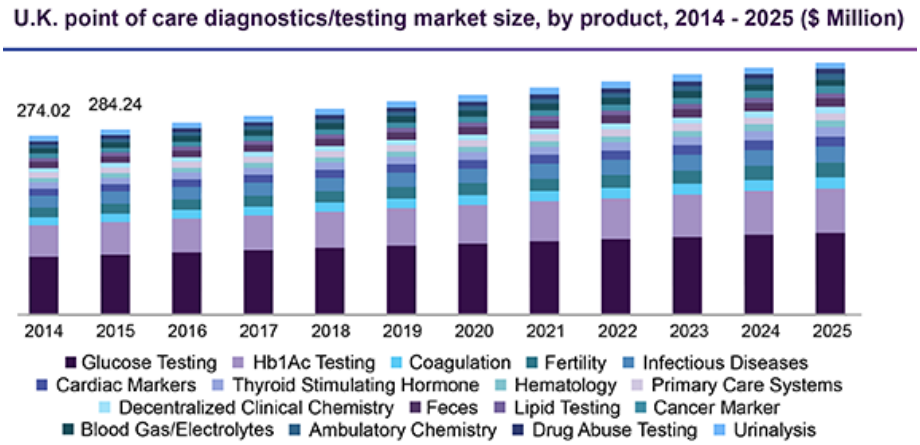

Figure 1: *U.K Point of Care Diagnostics/Testing Market by Size by Product, 2014-2025. POC testing market growth for glucose, infectious diseases, cardiac markers, hormones, cancer markers, and drugs of abuse.*

Criteria for POC Devices

The World Health Organization (WHO) has outlined criteria for evaluating POC devices in resource-limited environments. POC tests need to meet the ASSURED criteria (Affordable, Sensitive, Specific, User-friendly, Rapid and robust, Equipment-free, and Deliverable to end-users)[16]. Diagnostics that meet such criteria aim to provide same-day diagnosis and facilitate immediate decision making. In the case of POC HIV tests, quick results can increase the number of people knowing their status, assist in treatment, and determine if follow-up assessments and treatments are needed. Additionally, devices that require minimal training can alleviate the burden at testing centers and on the healthcare system. POC devices need to be operable in resource-limited settings, where there is unreliable electricity, non-sterile conditions, and a lack of trained personnel to perform a test.

Drawbacks and Criticism of POC Devices

While there are key advantages associated with POC testing, there are also flaws and criticisms that need to be addressed moving forward. From advancements in POC testing, readouts have transitioned to using handheld readers. In the case of handheld glucose meters, they are incomparable to lab test results despite their portability and user-friendliness[17]. These minor deviations can severely impact patients who are on strict glucose control plans. Since there are multiple methods of performing the same test, the lack of standardization can lead to inconsistent results. Even with a simple test, data management and oversight are complex and require training and proper assessment. Additional criticisms of POC include battery life, images are lower quality compared to laboratory instruments, tests can potentially be inaccurate or unreliable, tests may lead to false negatives, and there can be faults in the communication systems for sharing information. POC tests waived under the U.S Clinical Laboratory Improvement Amendments (CLIA) have a limited range of capabilities relative to full laboratory tests[18]. There can be a trade-off between the test's rapid format and its accuracy. Due to short test times, some clinicians believe that POC testing should be used as a screening tool rather than an on-site diagnostic since comprehensive tests can provide more accurate results.

Common POC Diagnostic Devices

Small devices for POC testing range from dipstick assays to cartridge-based devices such as chemical-based detection in agricultural monitoring, glucose testing, and drug immunoassays. A subset of portable devices uses fingerstick capillary

samples that are directly applied to POC instruments that perform rapid analysis and output the result on a digital display[19–21]. Another subset of POC tests, dipsticks, works without external devices and is applicable to resource-limited countries where such external devices may not be readily available. Dipsticks are the simplest form of POC technology, in which porous membranes are dipped in a sample liquid to perform a test. Dipsticks are usually made of paper with stored reagents that can be used to test liquids for a given analyte. There are dipsticks for testing urine samples for hemoglobin, urinary tract infections, glucose, and various proteins[22–24]. Some versions of dipsticks require more operator care since their performance is dependent upon sample volume and sufficient testing times for a final readout[25]. A similar version to a dipstick test is lateral flow immunoassay that offers fast test times and requires lower sample volumes.

The diagnostic analog of LFA in a central laboratory is the enzyme-linked immunosorbent assay (ELISA), which is a plate-based assay for the detection of analytes, antibodies, peptides, proteins, and hormones, among others. Fully automated instruments in laboratories around the world use the immunoassay for routine measurements of various analytes in patient samples[26]. Usually, an antigen or antibody is immobilized to a solid surface. An antigen is immobilized by surface adsorption or by capture on an antibody. After immobilization, the detection antibody is added, which can be covalently linked to an enzyme to produce a visible signal that is read by a plate reader. Between steps, the plate is washed with a detergent solution to remove any proteins or particulates that may bind non-specifically. While ELISA is performed

to evaluate the presence of an antigen or an antibody, it is a useful tool for food allergens, antibody concentrations, and blood tests. Various sample types can be used from urine, saliva, serum, plasma, and cellular and tissue extracts, among others. ELISA is a common technique due to its high sensitivity and specificity of detection. It is a high-throughput assay that can be done in a 96-well plate and even a 384-well plate. To detect the sample antigen or antibodies, various versions of ELISA exist from the direct, sandwich, and competitive assay (Fig. 2). However, it requires trained personnel and is time-intensive. ELISAs are used in the development of antibody pairs for LFAs. This helps in determining the best antibody pair for surface immobilization and reporter conjugation.

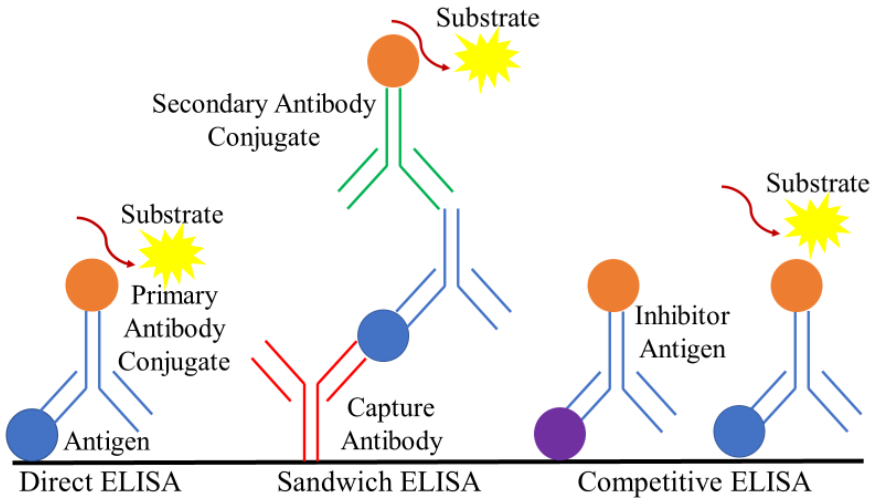

Figure 2: *ELISA Formats*

For a direct assay, the antigen of interested is immobilized by direct adsorption to an assay plate or by attaching a capture antibody to the plate surface. Detection is through an antibody specific for the antigen and is directly conjugated to horseradish peroxidase (HRP) or an enzyme that results in a colored or chemiluminescence

readout. As for a sandwich assay, the analyte is bound between two primary antibodies, followed by a secondary antibody conjugate that will result in the readout. Competitive ELISAs are used when the antigen is small and has only one antibody binding site. A labeled analyte in a sample competes with a labeled analyte to bind an antibody. The labeled unbound analyte is washed away.

With improvements in strip assays and electronic devices, one of the most well-known POC devices is the glucose meter. The biosensor is based on the catalytic action of glucose oxidase, by which an electrical current is generated that can be measured. Extensions of the glucose biosensor have led to continuous blood glucose monitoring[27]. Another meter-type device measures prothrombin time, the time it takes for plasma to clot. Calcium ions and thromboplastin (an enzyme released by damaged platelets) are added, and the time for blood coagulation to end is reported. It is used in the screening of coagulation disorders when clinicians report abnormal findings[28]. These tests are based on a rapid format and require external devices for proper performance.

Various POC devices use small cartridges that require two or three drops of blood added on a cartridge, which is then inserted into a handheld device. This is best exemplified by the i-STAT system (Abbott laboratories), which is a blood analyzer allowing results in as little as two minutes. Test results can be uploaded automatically and delivered wirelessly to storage systems. The cartridge utilizes thin-film sensors with microfluidics for the detection of various analytes from Na, K, lactate, pH, PO_2, and PCO_2, among others. This POC device has gained popularity due to the ability to

test multiple analytes on a single device, using different cartridges and the reliability of its measurements[29]. Personnel operating the equipment only need to understand one operating procedure, and process steps and handoffs can be eliminated to reduce errors and promote patient safety. Additionally, the device is an economical way of providing multiple results from a single test. Another handheld testing system is based on Smart Card technology in which biosensors and microfluidics are printed on a 35 mm tape[30]. The advantage of this technique is that it does not demand cleanroom manufacturing that is required for thin-film sensors.

Besides handheld devices, there are large bench-top devices that are used in centralized laboratories. Space is a premium in these laboratories, so the trend of miniaturization and increasing computing power is allowing the development of solutions to meet new needs. POC medical diagnostics must be accurate and sensitive enough to meet their clinical purpose. This is not always possible. For example, in the detection of hemoglobin A1c, which indicates the average level of blood sugar over the past two to three months, handheld devices have not been able to achieve the accuracy and sensitivity needed with low costs[31]. In this case, large bench-top analyzers are required to meet the analytical specifications. Various companies have specialization in this area from Siemens, Alere, and Roche with similar goals for their devices from having a simple user interface, test monitoring, and operating procedures. The advantage of bench-top analyzers is the ability to measure a wide range of clinical chemical analytes and perform multiple immunoassays. The

dominant application for bench-top testing is blood gas analyzers, which can measure various electrolytes, urea, creatinine, and glucose, among others[32,33].

Lateral Flow Assays

A major class of POC diagnostics is lateral flow immunoassays (LFAs), which are low-cost, simple, rapid, and portable. LFAs are porous-based platforms for the detection and quantification of analytes in complex mixtures. Samples are placed on a test device, and the results are displayed within 5-30 minutes. LFA-based tests are widely used for the qualitative and quantitative detection of analytes, antigens, antibodies, DNA, RNA, and biomarkers. A wide variety of biological samples can be tested from blood, urine, saliva, sweat, serum, plasma, and other bodily fluids[34–37]. The most common application of an LFA is for the detection of the pregnancy hormone, human chorionic gonadotrophin (hCG). While LFAs are predominantly used in the healthcare field, they are employed in other industries from animal health, agriculture, food safety, environmental monitoring, drugs-of-abuse testing, forensic science, pregnancy, and fertility testing. Thus, advancements in LFAs will allow contributions to various industries where rapid tests are needed for the screening of animal diseases, pathogens, chemicals, water pollutants, and toxins, among others.

Recent years have seen an increasing demand for POC diagnostic assays for the detection of multiple analytes. LFAs are easy to perform without laboratory oversights or individuals without training. They are easy to use, cheap to produce, and are accepted by users and regulatory authorities. A single LFA will only allow for the detection of one analyte, and in cases where a clinician requires more information to

make an informed decision, the detection of multiple analytes is useful. Multiplexing in LFAs is possible, allowing for the detection of numerous analytes[38]. In certain regions, various diseases are present with similar symptoms but do require different treatments. While novel technologies are being developed in the clinical diagnostic market and require billions of dollars and decades of work, the improvement and further development of LFAs often is a favorable alternative. The potential to produce devices that provide crucial information for challenging applications such as early cancer detection, disease monitoring, etc., is leading the growth for the POC market.

LFAs are well adapted for use in developing countries, small ambulatory care settings, remote regions, and battlefields. This stems from the fact that LFAs often have long shelf lives, and that refrigeration is not required for storage. From the development of LFAs to end-user testing, devices require a further examination for meeting the ASSURED criteria. A test that can provide reliable results from a naked eye may be better than a test that involves the use of a hand-held device. Concerns that need to be addressed can range from if the device is available in the country, can untrained personnel operate the equipment, the device cost, does the device provide low detection limits, data storage, device connectivity, among other concerns that need to be addressed based on the POC device.

The principle behind LFAs is that a liquid sample containing an analyte of interest moves along a porous membrane, usually paper or a wax substrate through capillary action. An analyte present in the sample moves through various zones of the strip, where it will interact with molecules already present on the strip. Specifically,

LFAs employ reporter particles that are transported by capillary wicking in a porous membrane, to binding sites for antibodies or antigens. LFAs most often employ antibodies attached to reporters as recognition elements, and their binding on the membrane is affected by the flow along the strip and the time they interact with an analyte and capture antibodies.

There are two different types of LFAs, which are a sandwich and a competitive assay. For the latter case, a positive test is represented by the displacement of a captured detection reagent with an analyte. Competitive assays are mainly used for small analytes, which are commonly seen in drugs of abuse[39]. Sandwich assays are common, and a positive test is represented by the presence of a colored line at the test and control line position. Both types of assays can be multiplexed, allowing for the detection of more than one analyte. Additionally, multiplexing offers cost-saving benefits and regions where resources are limited and can be done with multiple colored particles or using external readers. However, it is difficult in LFAs due to flow and possible interference that may arise from particles being captured at one line and not the other. If there are multiple lines where antibodies are immobilized on the membrane, this can complicate the flow and interaction of the analyte to the reporter particle and its subsequent binding at the membrane.

As the sample adsorbs at the beginning of the strip, it will wick from the sample pad, which in some instances contains a filter to ensure an accurate and controlled flow of the sample (Fig 3). Depending on the sample, the rate at which liquid enters the sample pad and flows to the conjugate release pad is crucial for an

accurate LFA result[40]. The critical role of the sample pad is the flow and even sample distribution to the conjugate pad. Detergents, surfactants, and blocking agents may be used to treat the sample pad to alter the samples' viscosity, so there is an increased reaction time at the conjugate release pad or chemical modification for the sample to bind at the test line.

The conjugate pad stores antibodies that are specific to the analyte, and are conjugated to reporter particles. The sample, along with the conjugated antibody bound to the analyte migrates along the strip towards the membrane. Some have incorporated an additional membrane to extend the interaction between antigens and antibodies to enhance the test's sensitivity[41]. Different proteins, detergents, and surfactants can be added to the sample pad but mainly the conjugate pad to promote solubilization of the conjugate and minimize non-specific binding of proteins along with reducing the adsorption of the analyte to the membrane[42].

As the sample migrates towards the membrane, it will interact with specific biological components, which are usually immobilized antibodies or a recognition element. Immobilization is through passive adsorption, or recognition elements are chemically linked to the porous membrane. There are two lines, a test, and a control line, which have different sets of antibodies (Fig. 3). At the test line, antibodies will be specific for the analyte of interest, while the control line will bind to an antibody conjugated to the reporter particle. Recognition of the analyte results in an appropriate response on the test line while proper liquid flow indicates a response on the control line.

The sample will pass through the rest of the membrane, into the last part of the strip, the absorbent pad, which will absorb any excess sample. Membranes can differ on the type of reporter particle to ensure a controlled flow. Absorbent pads will vary based on the volume of the sample test required to yield an accurate result. Between each part of the strip, there needs to be a proper overlap of the membranes. If the overlap is altered, this is known to affect the flow along the strip and reduce the sensitivity of the assay. This is pivotal for the conjugate release pad. The overlap of the sample pad to the conjugate release pad and the conjugate release pad overlap to the membrane is important since the release of the conjugate, and its initial flow will determine its trajectory along the strip.

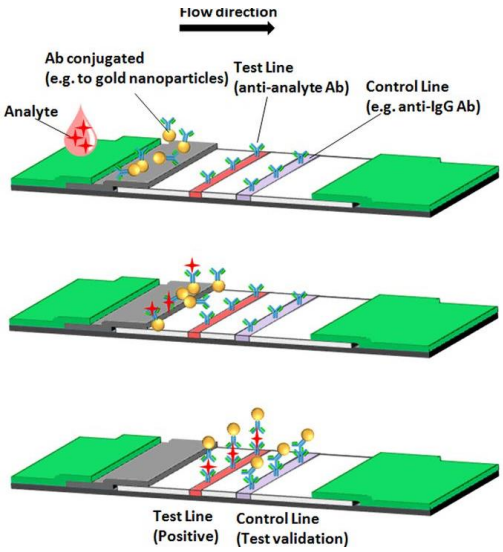

Figure 3: *Components of a Lateral Flow Strip.*

The sample pad, conjugate pad, membrane, and absorbent pad (Fig. 3). A sample medium is added at the top of the sample pad that flows through the strip. An analyte present flows through the strip and binds to the conjugated reporter particles,

which then migrates along the strip and binds to anti-analyte antibodies immobilized on the membrane. Excess liquid is wicked by the absorbent pad[43].

Reagent transport, analyte, and reporter interaction, flow rate, and signal generation can affect the sensitivity of LFAs. Sensitivity is reduced by a high level of noise, or high background from incomplete transport, such as non-specific binding of reporter particles or detection reagents. The reporter particle or detection reagent may immobilize at and around the test line, leading to signal noise and affecting the sensitivity of the assay. Additionally, there can be reduced sensitivity in clinically relevant samples such as blood, saliva, and urine due to non-specific binding of detection reagents, reporter particles, or by interferents present in the sample. A strategy for minimizing non-specific binding is to use blocking reagents. These reagents can be dried onto the strip during LFA development or incorporated into the buffer when running the LFA strip. Blocking reagents currently used in LFAs are bovine serum albumin (BSA), casein, antibodies, or serum. These reagents have been developed further to improve sensitivity in LFAs.

Another strategy to reduce non-specific binding and ensure constant flow in LFAs is the use of detergents and surfactants. During development, strips can be treated with these reagents and are also used in the running buffer for LFAs. Treating the strip with surfactants can reduce possible negative interactions from salt concentrations, pH, protein compositions, or any molecules that may cause non-specific interactions in clinically relevant samples[44]. Additionally, these can improve flow and enhance the reproducibility of the assay. Strip treatment and the buffer used

while running the LFA need to be optimized for each test. Changes in the buffer pH and salt concentration can have drastic effects on the capture and subsequently affect the sensitivity of the assay. Furthermore, strip treatment and buffer optimization may also need adjustment based on the sample being used, such as whole blood, urine, or saliva. During LFA development after the strip is treated with the selected mixture of detergents and blocking reagents, the strip needs to thoroughly dry overnight in a desiccated environment (< 20% humidity). In some instances, drying at 37 ℃ or higher for a short period may be required before a transfer to the desiccated chamber. LFA strips can absorb moisture, and this can lead to destabilization of reagents dried on the surface, such as the immobilized antibodies[45]. Additionally, if the strip takes up moisture, this will affect the flow along the strip and can affect capture and alter the sensitivity of the assay, so dry handling and desiccated storage is crucial for sensitive LFA performance.

Antibody Selection for LFAs

Antibody selection plays a crucial role in the sensitivity of an assay. There are two main forms of antibodies, polyclonal and monoclonal. Polyclonal antibodies are mixed immunoglobulins which are secreted against a particular antigen, produced by different clones of plasma B cells. They can interact with different epitopes on the same antigen. Monoclonal antibodies are produced by a single clone of plasma B cells and interact with only a particular epitope of an antigen. Polyclonal antibodies are easier to couple to labels[46]. However, since they are a heterogeneous antibody population, there is batch-to-batch variability, and there is a likelihood of cross-

reactivity due to recognizing multiple epitopes. As for monoclonal antibodies, there is an unlimited batch-to-batch reproducibility, a high specificity since recognition is for a single epitope, and thus a lower chance for cross-reactivity[47]. They can be susceptible to changes when conjugated to a particle. For LFAs, usually, the polyclonal antibody is conjugated to the reporter particle, and s monoclonal antibody is immobilized to the membrane. However, in LFAs, this arrangement is switched depending on the sample media and the analyte being detected. For each LFA, antibody pair optimization is a crucial first step for developing a sensitive assay.

Sensitivity, Specificity, and Limit of Detection

Metric for LFAs and diagnostics are clinical sensitivity, specificity, and the limit of detection. Sensitivity is the ability of a test to detect the analyte when it is present, or in a broader sense, the proportion of individuals who test positive for disease among those who have the disease. A test that exhibits high sensitivity is reliable when the test is positive, assuming high specificity, and when it is negative, there is rarely a misdiagnosis with high sensitivity; however, this can be different if the test has low specificity. Specificity is the ability of the test not to report the analyte if it is not present. In a clinical sense, this is the proportion of individuals who do not have the disease test negative for it. If a test didn't have high specificity, an assay might falsely indicate an individual has a particular condition, and treatment would start when it is not needed. For certain diseases, starting treatment if an individual does not have a condition can be detrimental to their health. So, an LFA would ideally have high sensitivity (>95%) and high specificity (>95%)[44]. Another metric are

positive and negative predictive values, which are the proportion of positive and negative results that are true positives and true negatives. The values depend on prevalence, which is the proportion of the population found to be affected. Large pools of diverse populations for biomarker selection and detection plays a crucial role in LFA development. Another metric for LFAs is the limit of detection, which is the lowest analyte concentration that can be detected and distinguished from the background signal. To determine the detection limit, multiple samples need to be tested to determine the background signal and assess the detection of various analyte concentrations. For the background signal, the mean value and standard deviation are calculated. The limit of detection is set as the background signal plus 3 times its standard deviation, through variations of this approach have used, 1, 2, 4, or even 10 standard deviations[48]. The aim is that in the presence of an analyte, a test will produce a signal greater than the noise in the absence of an analyte.

Reporter Particles in LFA

Various LFA reporters have been employed, such as colloidal gold, colored latex particles, phosphors, magnetic particles, carbon nanotubes, aptamers, nucleic acids, or virus particles[44,49–52]. Reporter selection is one of the most critical decisions during the development of new LFAs, as it will impact the sensitivity, specificity assay's cost, developmental time, stability in the clinical sample, and whether or not a reader is required for the final LFA readout. LFAs must give accurate and reproducible results, so the reporter particles must be of high quality and well characterized. The reporter particle material used should be detectable at low

concentrations and retain its properties when conjugated to antibodies or biomolecules. Ease of conjugation with biomolecules and stability over long periods are desirable features of a reporter particle. Reporter particles may generate a direct signal, such as a colored spot, while others require additional steps to produce a signal, such as enzymes reacting with a suitable substrate. Particles that provide a direct signal are preferable for test simplicity and reduced assay time. The reporter particle determines how the signal is presented to the final user, which especially applies to remote locations in the developing world. Some applications use mobile phones or other telemedicine applications for the final readout. In other cases, the test result may be transmitted to remote personnel with expertise that can interpret the result and guide treatment.

Colloidal gold nanoparticles, the most commonly used reporter particles in LFA, are inert and almost perfect spherical particles. They have a high affinity towards biomolecules and can be easily functionalized. Depending on the size and shape of the particle, the optical properties will differ. Additionally, the particles are well characterized for use in LFAs. Another common form of particle used is magnetic particles, which can be measured by an optical strip reader[53]. Furthermore, the magnetic signal from the particles can be used as a form of detection signal with a magnetic reader. Magnetic signals are stable for longer times compared to optical signals, with enhancements of sensitivity from 10 to 1,000-fold. Magnetic particles can demonstrate an absorption spectrum that covers the whole visible region. However, magnetic particles can aggregate in the porous membrane of the LFA strip,

and external magnetic fields can assist in particle relocation from depths of the LFA strip to more-visible locations nearer to the top surface producing a more visible signal[52].

Other common reporter particles employed in LFAs are latex and cellulose beads. Both these particles are developed commercially and have easy bioconjugation techniques that are well established. They provide colorimetric signals with multiple colors available for the detection of various analytes. Cellulose and latex beads have large diameters (200 nm or greater), which works well for certain assays but can cause aggregation, so the addition of a surfactant may be needed.

Fluorescent and luminescent particles are widely used in LFAs since fluorescence can allow for quantification of the analyte concentration. Organic fluorophores such as rhodamine are used, but a key problem is photobleaching resulting in reduced sensitivity. Additionally, they can chemically degrade. With advancements in nanomaterials, quantum dots (QD) display unique optical and electrical properties. As with gold particles, QDs show size-dependent optical properties, and only a single light source may suffice for the excitation of different QD sizes. They have high photostability and absorption coefficients but can have surface defects affecting the quantum yield[54]. For the implementation of QDs in LFAs, an external device would be required. Another fluorescent particle is upconverting phosphors (UCP), which gives emission in the visible region upon multi-photon excitation in the infrared region. Additionally, they do not show autofluorescence and do not photodegrade biomolecules[55]. Moreover, they are produced easily from bulk

materials; however, this can affect their uniformity, and the labeling of UCP reporters requires multiple steps. In certain assays, UCP demonstrates size-dependent sensitivity and specificity. Other fluorescent particles are europium (III) chelate nanoparticles, which have shown higher sensitivity than gold nanoparticles but require external devices[56]. Additionally, persistent luminescence nanoparticles offer enhanced sensitivity through time-resolved measurements and exhibit a sensitivity an order of magnitude lower than colloidal gold[57].

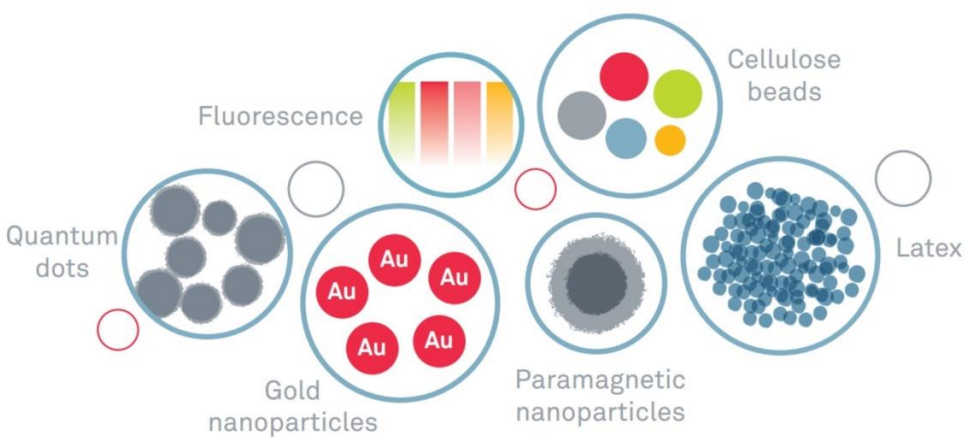

Figure 4: *Various Reporter Particles. Employed in LFAs, ranging in size of 50 to 1000 nm*[58].

LFA Readouts and Readers

Readouts for LFAs vary based on the reporter particle, if external devices are employed, and ranged from colorimetric, magnetic readings, light-based, and spectral based readouts. Most conventional LFAs that have been designed generate a color signal that can be read by the naked eye, without the need for an instrument. A color readout is user-friendly and straightforward but can cause difficulties of interpretation due to differences in the perception of color between individuals, the effect of age, and

visual ability. The development of handheld readers can allow tests to switch from a semi-qualitative assay to a quantitative result that will support clinical decision making. With a trend towards portable and wearable technology, the lateral-flow strip is being driven towards instrumental interfaces. This will allow it to be connected to the "internet of things" and interface with large data systems. Through this, real-time data will enable contributions to the medical and environmental database for monitoring spreads and outbreaks of various scenarios such as diseases, water quality, and bioterrorism, among others. However, with the sharing of real-time data, privacy becomes a concern. Whether and how the data is shared, how the information is collected or stored, and if there are regulatory restrictions are concerns, society will need to address.

For visual readouts, various commercial optical readers are available based on reflectance or fluorescent principles. These readers can convert the readout into a digital result. Handheld detectors are allowing the transition of assays from qualitative to quantitative tests enabling LFAs readouts to have more precise results. The addition of software with data analysis allows for further enhancements of LFA tests, and data storage can allow for tracking health data and personalized healthcare. An extension of handheld devices used for quantitative analysis are imaging systems. Lateral flow strips can be imaged by a high-density charge-coupled device (CCD) or complementary metal-oxide-semiconductor (CMOS) camera that can capture the test and control lines on the membrane[59,60]. When combined with data analysis, calibration curves, and statistics, this can allow for further quantification. An advantage of

imaging systems is their adaptability to a variety of tests with various labeling systems. For rapid test analysis, some systems using scanning optics that will analyze only the membrane, instead of the full strip. When using imaging, Raman techniques were used with a 1,000-fold increase in detection sensitivity for the Flu B assay using gold nanoparticles labeled with Raman reporters[61]. However, while this is an example where Raman imaging can provide increased sensitivity, but it comes with a high instrument cost. The end-user, along with the environmental conditions, must be considered. If an immunoassay uses a high-cost reader that allows for higher sensitivity, fewer can be employed due to cost. If the test is cheaper, sensitivity may be sacrificed, but the test can be employed in more areas. The practicality and cost of the test need to be considered during the development of an LFA. Additionally, this ties in with where the LFA is going to be primarily used, as certain features can be implemented or not, whether it is in a developed or developing country.

To address challenges with handheld readers and their developmental costs, the mobile phone is an emerging platform due to its practicality and ubiquity. With the advancement of mobile phones, they have become a diagnostic platform that can be used for imaging, data processing, storage, display, and communication. There are more than an estimated 6.5 billion cellphone subscriptions, making them an attractive platform for diagnostics. Cellphones are equipped with CMOS cameras and have low power consumption and can provide high image quality. Cellphones biosensing often can match the analytical performance of delicate instruments[62]. Various researchers have demonstrated the use of a phone camera as an optical reader, while others have

3-D printed attachments for the camera to fit various LFA tests[51,63–65]. Due to different cellphone brands and editions on the market with increased technological advancements, variability in imaging processing for LFA purposes remains an issue. Furthermore, phone software updates may affect the application or analysis being performed. Others have demonstrated increased sensitivity using a mobile phone through optimization of the incident light, and the angle of detection through Mie and Rayleigh scattering[59]. The results can be stored or sent to a server for further data analysis and evaluation. Overall, the trend is moving towards the integration of optical instruments from handheld devices to mobile scanners allowing for a variety of home-based diagnostics and the growth of decentralized healthcare.

LFA readout results have also been measured through electrochemical sensors that allow for high sensitivity. Electroactive labels have been implemented along with electrodes for electrochemical detection[66]. Voltammetric detection does not allow for real-time measurements, but there is current work being performed to reduce the number of steps and allow for such measurements[67]. Others have worked on using chemiluminescence readers, which can be used for a broad range of analytical applications. Chemiluminescence assays usually require an external imager, and the assay may require complex reagents which need to be stored at low temperature or reagents that need to be mixed before the assay. It has been demonstrated that chemiluminescence signals can be captured by a CCD or CMOS camera through an external device or using mobile phones. Using a chemiluminescent readout, sensitivity was improved as much as 1,000-fold for the detection of hCG compared to colored

gold nanoparticles[68]. Additionally, others are working on self-contained assay systems, so the addition of reagents that need to be stored at low temperatures or mixed could be removed from the assay procedure[69]. The same issues are being addressed when the readout may use a spectral imager or a magnetic reader. While one may reach the desired sensitivity for the assay during development, a concern remains if the test is practical and cost-effective for the area, whether it's in a resource-limited or a developed country.

The readout result and its subsequent detection can be traced back to the reporter particle and labeling system employed. Thus, reporter particle selection is crucial as it will play a key role in determining if an external device is required if trained personnel are needed to perform the test, practicality, and cost-effectiveness of the test. While LFAs can vary in terms of their reporter particles and readout, they generally suffer from being qualitative tests, which provide a yes or no result. In cases where precise results are required, centralized laboratory instruments are used while LFA development works on providing quantitative results.

Viral Nanoparticles as LFA Reporters

The implementation of various reporter particles and different readout methods for LFAs have been mainly aimed at improving the assays' analytical sensitivity. Techniques such as pre-concentration to increase the assays' sensitivity have led to decreases in the detection limit[70]. Another approach to enhancing sensitivity is conjugating enzymes to reporter particles, which also demonstrated a reduction in the limit of detection[71]. In the detection of viruses and disease, LFAs have lagged behind

more elaborate laboratory methods from PCR and enzyme-linked immunosorbent assays (ELISAs). Bacteriophage peptides have been reported to be suitable as affinity reagents in ELISAs. This stems from phage display, which allows for the study of protein-protein, protein-peptide, and protein-DNA interactions[72]. A gene for a protein of interest is inserted into the phage coat protein, which causes the phage to display the protein on the outside coat protein. The displaying phages can be screened against other proteins, peptides, or DNA sequences. M13 bacteriophage is used for phage display and is reproduced in *Escherichia coli* but can attach to other bacteria to inject its genetic material into the bacterial cytoplasm. M13 injects the viral DNA strand (+) in the cytoplasm of *E.coli* where a complementary strand (-) is synthesized and forms a parental replication form. This is then nicked and creates a circularized displaced viral DNA strand (+). A pool of double-stranded replicative form is produced, where the negative strand of the replicative form is the transcription template, and mRNAs are translated into phage proteins. Additional, phage proteins are synthesized or inserted in the cytoplasm and are part of the DNA replication process.

Functionalized viral nanoparticles have been explored in recent years for use as reporters in immunoassays, resulting in higher sensitivity and lower limits of detection. A bacteriophage, M13 phage, in particular, has been modified with recognition elements, reporter elements, and has been successfully used for diagnostics, medical, and imaging purposes[73–75]. M13 phage is filamentous with a length of approximately ~900 nm and a width of approximately 6.6 nm. M13 contains a core of circular single-stranded DNA encapsulated by 2,700 copies of the major coat

protein with minor coat proteins at the tips of the phage. The structure of an M13 bacteriophage is advantageous in lateral flow due to its high surface-area-to-volume ratio (Fig 5). Its surface consists of multiple copies of identical coat proteins and allows for chemical modification, allowing for its wide adaptability as reporters in the use of LFAs. Due to the surface area available for conjugation, there are hundreds of binding sites for reporters and antibodies, even if mutual steric exclusion is considered. Another advantage of M13 phage is that they are stable over a wide range of pH, temperatures, and environmental conditions.

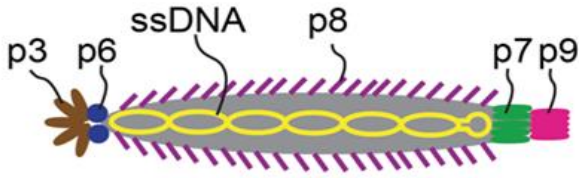

Figure 5: *Structure of an M13 Bacteriophage. Showing the different coat proteins which can be modified.*

Others have demonstrated using M13 as molecular scaffolds or optimizing their protein coat, which changes depending on the solution pH and salt cocnentration[76,77]. The coat protein is suitable for a range of chemistries and can also be genetically modified. Thiol-maleimide and N-hydroxy succinimide ester chemistries have been adapted for M13 bacteriophage. Through this, M13 can be linked to antibodies, small molecules, enzymes, nanoparticles, and a variety of functional groups. While phage is stable in a range of conditions, any chemical conjugation or element being conjugated can degrade over time, so the stability of

phage conjugates further characterization. Additionally, phages have advantages in that they do not normally infect mammalian cells, as there are no receptors on these cells for phage. Also, as mentioned, genetic modifications are possible through phage display, so the ability to display selective ligands for binding is possible. Bacteriophages have been used in the medical field for therapeutic administration to treat bacterial infections, with minor side effects[78]. They have been administrated topically, subcutaneously, orally, intranasally, and intravenously. There are high levels of phage in the digestive tract and the natural environment. It also has been reported that bacteriophage can be found in water treatment plants, bodies of water, and soils, among others[79]. The discovery of new phages is leading further research into phage display and screening for new proteins, peptides, and DNA segments. Phages have additional benefits and were approved by the U.S. Food and Drug Administration as an antibacterial food additive.

The development of alternative LFA reporters that provide an increased sensitivity is of great interest. Previously we introduced engineered M13 bacteriophage particles as reporters in lateral flow assays that resulted in a 100-fold greater sensitivity in the detection of human chronic gonadotrophin (hCG) with the same antibodies compared to gold nanoparticles[49]. M13 was incorporated into LFAs for the detection of virus-like particles (VLP) for norovirus, which is responsible for gastrointestinal disease. Compared to a gold nanoparticle LFA, the limit of detection was improved 100-fold using bacteriophage reporters[50]. Horseradish peroxidase (HRP) and target-specific antibodies can be chemically attached to the coat protein (pVIII) of

M13. From previous studies, M13 reporters demonstrated success in LFA with low antibody loadings, eliminating binding by any possible confounding effects of multivalent binding by multiple copies of the target-specific antibody[80]. Additionally, it was reported that M13 phage could display small numbers of antibodies and a maximal number of enzyme reporters.

Another key advantage of why M13 phages are attractive LFA reporters is that they have evolved under Darwinian selection so that they exhibit low non-specific binding[81,82]. This allows an improvement in LFA sensitivity by increasing the signal-to-noise ratio at low analyte concentrations. Reporters or analytes present in the sample that flow along the strip may bind or not at the target-specific site. The non-specific binding will affect the readout of the LFA and will yield a high background, making it difficult to discern the signal from binding at the specific site. To address and mitigate these issues, the addition of surfactant can be used. Such compounds reduce surface tension, and commonly used detergents for LFAs are Triton or TWEEN coupled with BSA. This will allow a faster flow of the analyte and reporters and minimize non-specific binding. In some instances, LFA strips will need to be pre-treated with a surfactant in case the sample or reporter particle is known to bind non-specifically or if it will get caught in the pores of the membrane. Additionally, if the presence of an analyte is too high, the test may yield a false-negative result. This can also arise from antibody interference, cross-reactivity, and signal interference. Surfactants have been known to mitigate this issue. A known issue in immunoassays is the hook effect, which results in false negatives from high analyte concentrations.

Excessive antigen binds to sites on the capture and detection antibodies, preventing the sandwich formation, causing a reduced detection.

Due to M13's high sensitivity for the detection of hCG and VLPs for norovirus, it is of interest to pursue further optimization to reduce the number of hands-on steps. Additionally, bacteriophage deserves further characterization in terms of its chemical modification, antibody capture, flow analysis, and storage. M13 phage will be characterized through the lyophilization of LFA strips, such that we will be able to further validate the use of M13 as a reporter in long term storage and clinically relevant samples.

Binding of Particles in LFA

Binding within LFA is affected by the flow of liquid along the strip the time reporters interact with an analyte and capture antibodies, and the inherent on-rate kinetic of the association. Vertical-flow immunoassays and a variety of biosensing technologies, as well as various preparative methods, also involve the capture and flow of targets and reporters in porous matrices. Mathematical models are being used to understand and improve the performance of LFAs[42,83–85]. Measurement of the kinetics of interaction and capture in lateral flow matrices has been difficult, especially on time scales below one second. The performance of LFAs can be improved by adjusting the assay parameters, including reporter particle, fluid velocity, reagent concentration, and the type of membrane. Increasing the analytical sensitivity of LFAs and its quantification would expand their usefulness across a variety of fields.

Current Techniques for Measuring Binding of LFA Reporters

Previous techniques aimed at measuring binding such as surface plasmon resonance, (SPR), biolayer interferometry (BLI), or stopped-flow fluorescence are not capable of providing measurements in porous matrices. SPR occurs when polarized light hits a metal film at an interface between materials with two different refractive indices. The method works by the excitation and detection of the oscillation of free electrons. When a light beam hits a metal film, the reflected beam is collected and analyzed. The reflected beam has an angle of reflection and a surface plasmon angle, which indicates the reflection and absorbance signal. The reflection and surface plasmon resonance angle may represent a molecular binding event occurring on or near the metal film or a conformational change in the molecules bound to the film. This optical technique allows molecular interactions to be studied in real-time without the use of labels. SPR technique has applications for LFA development, by measuring the interaction of an analyte with antibodies and reporter particles, and vice versa. However, in SPR, one biomolecule is chemically attached to the metal film, and the interaction with the bound biomolecule is measured[86]. For example, if an antibody was chemically bound to the metal film, and one was measuring the interaction with an analyte, SPR serves as an important tool measuring for this interaction. However, the lateral flow of analytes is not possible. Additionally, the environment is different in LFAs, in which molecular interactions occur in porous matrices. For understanding the molecular interactions based on flow in porous matrices, SPR is not the proper technique. Biolayer interferometry is a label-free optical technique based on the

interference pattern of light reflected on surfaces. There is a layer of protein immobilized on the biosensor tip and a reference layer, so any change at the biosensor tip, such as the number of molecules or binding can cause a shift in the interference pattern that can be measured in real-time[87]. Again, molecular interactions occur in different environments with LFAs, so the results would not directly apply to capture in LFA.

Stopped-flow fluorescence allows for studying fast chemical reactions in solutions. Two solutions are loaded into syringes and then suddenly pushed into a mixing chamber. The chamber is linked to a switch that triggers a measuring device, and the flow is stopped suddenly and measured. Stopped-flow is mainly used for association and dissociation kinetics, and antigen/antibody interactions[88]. To measure the interaction, various forms of spectroscopy and scattering of radiation are used. With this technique, interactions between analyte and antibody are possible but still doesn't address the capture in a porous matrix.

Binding of Viral Nanoparticles in LFA Matrices

We have demonstrated there are varying orientational binding modes for M13 in LFA matrices, and how its binding is affected by the liquids' viscosity and its length[80,89]. Analysis of these binding modes was performed in Fusion 5, which is a silica fiber porous membrane. For M13 phage binding to the anti-M13 antibody, binding occurs on its lateral coat protein side and happens immediately after phage collides with a silica fiber within the membrane. The other binding property characterized was the capture of tip-biotinylated phage to NeutrAvidin. Avidin has a

very high affinity for biotin molecules and is stable and functional over a wide range of pH and temperature. Through this capture mechanism, phage only tip-bind due to the biotinylation of the p3 tail protein[89]. The local flow re-orients the phage allowing them to align parallel to the fiber before binding[89]. From these studies, the shape of phage may promote binding by increasing the capture cross-section and reorienting in lateral flow for an increased likelihood of capture.

As described above, M13 phage has demonstrated high sensitivity in LFAs, and the phage shape couples to the membrane and promotes reorientation for binding. It was hypothesized that capture could be increased by adjusting the size and shape of the reporters. This was investigated with Alexa 555-labeled biotinylated phage and its capture to NeutrAvidin. Three filamentous phages of varying dimensions were examined, potato virus M virus-like particles, PVM, (200 nm in length, and a 13 nm width), M13 (900 nm length and a 6 nm width), and wild type filamentous Pf1 bacteriophage, Pf1, (2,000 nm length and a 7 nm width)[80]. The capture on LFAs was visualized with a fluorescent microscope. Through these studies, regions with faster local flow had more phage bound, indicating that higher average local flux increased binding. The aspect ratio of phage was investigated to determine how it affects binding. The number of bound phages increased with the aspect ratio and scaled with the phage surface area, indicating the binding interaction may be influenced by the number of recognition elements on the surface. Thus, the greater space for recognition elements on the coat protein of phage allows it to encounter the membrane fibers and enhance the assay binding efficiency. These experiments were performed with Fusion

5, which differs from nitrocellulose membranes. For nitrocellulose membranes that exhibit faster flow rates, the assays are less sensitive. This may be different with phage due to its aspect ratio, as it couples with fluid flow and tumbles through the strip in Fusion 5. While this needs further investigation, it reflects that reporter particles and flow rates can differ depending on the membrane and alter the sensitivity of the assay.

The transport of viral nanoparticles along a porous membrane (Fusion 5) strip driven by capillary force has an estimated average velocity of 1.8 mm sec^{-1} in phosphate-buffered saline (PBS)[89] measured at the membrane. In a typical test strip, the test line is 1 mm wide, and thus the residence time of phage passing the capture line is 0.5 sec. To measure capture in LFAs, varying the fluid flow has been challenging and has used viscous solutions to slow the rate. The ability to control the rate is essential to understand capture under 0.5 seconds, and this is possible through a vertical flow format. It is evident that a further understanding of the interaction between M13 bacteriophage and binding to recognition elements at short time scales is needed.

To further understand the enhanced sensitivity of M13-based LFAs, we examined the capture and flow of bacteriophage in porous membranes in a vertical flow format. While the flow direction is different for each assay, key insights on reporter and analyte binding can be gleaned on how to improve such assays. It is essential to have a range of biochemical, biophysical, and chemical techniques available to characterize analyte and novel reporter binding to recognition elements. To measure reporter capture, vertical flow allows greater versatility in changing the

flow speed enabling a way to discern how binding is affected by the flow. The flow speed can be adjusted to match the transit time of reporters at the capture line in lateral flow assays. Residence times of reporters through the membrane is possible in the millisecond time range allowing capture on short time scales. This opportunity represents a way to measure analyte capture in porous matrices in flow-through assays, in which reagents flow in the vertical direction. The performance of flow-through assays can be influenced by the membrane pore size and fluid flow, and signal intensity can be limited by the association rate of the affinity reaction[90,91]. The ability to measure how novel reporters bind in porous membranes with varying pore sizes and at fast flow rates can lead to insights on how to improve sensitivity in LFAs and flow-through assays.

Here we introduce rapid filtration, as a method for measuring the capture of analytes and reporters in porous matrices, and describe its use in investigating ultra-sensitive LFAs using filamentous bacteriophage as reporters. Previously, the rapid filtration technique was used for time-resolved measurements[92–96]. As discussed earlier, stopped-flow methods are restricted to cases where the molecular interaction being examined is optically active or can be stopped by an inhibitor. The rapid-filtration technique does not suffer from these limitations. The technique allowed for time-resolved measurements of calcium binding to ATPase, and it was possible to measure transport or binding process at short times, 10 to 20 msec[92]. The advantage of rapid filtration is the study of soluble proteins that can be immobilized or adsorbed in a porous filter. Any porous filter can be used and broadening the applications for this

technique. This allows one to measure the molecular interactions in a porous membrane, yielding insights applicable to LFAs. The flexibility of this method allows for further understanding of various analytes, reporters, and proteins, and how their capture is affected by flow in porous matrices. The sensitivity of M13-based LFAs can be examined by measuring M13 capture by varying the flow rate and times at a time scale under one second, allowing us to further understand the increased sensitivity of phage-based LFAs.

CHAPTER 2: RAPID FILTRATION APPARATUS FOR SUB-SECOND ANALYSIS OF ADSORPTION IN POROUS MATRICES

Introduction

A major class of point-of-care (POC) diagnostics is lateral-flow immunoassays (LFAs), in which antibody-bearing reporter particles are transported by capillary wicking in a porous membrane to capture antibodies. Reporter binding efficiency is affected by the rate of flow along the strip, and the time for interaction with an analyte with capture antibodies. Other technologies, such as vertical-flow immunoassays, a variety of biosensing technologies, and various chromatographic methods, also involve the capture and flow of targets and reporters in porous matrices. Mathematical models are being used to understand and improve the performance of LFAs, but measurement of the kinetics of interaction and capture in porous matrices has been difficult, especially on time scales below one second[42,83–85]. Most methods of measuring binding kinetics, such as surface plasmon resonance (SPR), biolayer interferometry (BLI) and stopped-flow fluorescence, are not applicable to porous matrices. One measurement technique potentially applicable to fibrous matrices is rapid filtration, used initially to measure binding of ligands to surface receptors on cells supported on a porous membrane. Previously the rapid filtration technique was used for time-resolved measurements of calcium binding to ATPase, the kinetics of phosphate-phosphate exchange mediated by an inorganic phosphate carrier, binding of nonionic detergents to membranes measurements of the kinetics of ADP and ATP transport, and calcium release from cell organelles[92–96].

The development of novel immunoassay reporter particles in immunoassay with lower limits of detection is a critical need. M13 phage, in particular, has been modified with recognition elements, reporter enzymes, and has been successfully used for diagnostics, medical, and imaging purposes[73–75]. We introduced engineered M13 bacteriophage particles as reporters in lateral-flow assays with a 100-fold greater sensitivity in the detection of norovirus and human chorionic gonadotrophin (hCG) when compared to conventional gold nanoparticles[49,50]. By fluorescence microscopy of labeled phage in LFA matrices, we demonstrated that there are several orientational binding mode's for M13, and how its binding is affected viscosity and phage length. M13 phage captured by polyclonal anti-M13 antibodies binds immediately after colliding with a membrane fiber, regardless of orientation[89]. However, when end-biotinylated phage is captured by Neutravidin, phage bind only after reorienting and transporting along the membrane fiber axis[89]. The wicking of fluid along a porous Fusion 5 silica membrane by capillary flow has an estimated average velocity of 1.8 mm/sec on the membrane portion of an LFA strip in phosphate-buffered saline (PBS) which, for a typical 1 mm test line, gives a capture residence time of 500 msec. The performance of flow-through assays can be influenced by the membrane pore size and fluid flow, and signal intensity can be limited by the association rate of the affinity reaction that occurs at short time-scales so measurements at such times is of great importance.[97].

Here we introduce rapid filtration as a method for measuring the capture of analytes and reporters in porous matrices on short time scales and describe its use in

investigating ultra-sensitive LFAs using filamentous bacteriophage reporters. The flexibility of this method should allow for further understanding of a broad range of analytes, reporters, and product, and how their capture is affected by flow in porous matrices.

Materials and Methods

Culture and Titering of M13 Bacteriophage

M13 phage displaying the Avi-tag, a substrate peptide for biotin ligase on the p3 tail protein, was a gift from Dr. Brian Kay (The University of Illinois at Chicago). Culture and titering of M13 phage were performed as described previously[97,98]. Avi-Tag-M13 was pre-mixed with *E. coli* TG1 culture for two hours at 37°C and was transferred to 2x yeast extract and tryptone (2 x YT) broth medium for overnight growth at 37°C. Bacteria were separated from the lysate by centrifugation (30 min, 3,200 *x g*) followed by filtration through a 0.45 µm filter (Corning, #430512). Phage were then precipitated using PEG/NaCl as previously described[99]. Phage titers were determined on X-Gal/IPTG plates, as described.

AviTag M13 Phage Coat Protein Biotinylation

Avi-tag M13 are further biotinylated on the p8 coat protein with N-Hydroxysuccinimide (NHS) biotin esters. 10 mM Sulfo-NHS-LC-Biotin (Thermo Scientific 21336) was mixed with 100 µL of M13 phage (10^{12} pfu/mL) to achieve 100 biotin molecules per phage particle. After a 30-minute incubation on ice, excess biotinylation agents were removed from the biotinylated phage solution with a 7 KDa molecular-weight cutoff (MWCO) Zeba Spin Desalting Column.

AlexaFluor 555 labeling of biotinylated M13

Biotinylated AviTag-M13 phage was labeled with AlexaFluor 555 NHS Ester (Life Technologies #A-20009) on the primary amines of the p8 major coat protein as previously described[100]. 100 µL of phage suspension (10^{12} pfu/mL) was added to a 7 KDa MWCO Zeba spin desalting column, and after centrifugation, the phage suspension was mixed with 5 µL of 10 mg/mL Alexa 555 fluor and incubated overnight at 4°C. To remove the unconjugated Alexa 555 fluor molecules, the solution was dialyzed against 1 L of PBS using a Float-A-Lyzer 300 KDa MWCO dialysis cartridge with five complete buffer changes over 36 hours.

Rapid Filtration Apparatus

A stainless-steel porous support (Fig. 6) is located directly below a stainless-steel syringe with an air gap of 2 mm. The porous support rests on a solenoid actuator that, upon activation, brings the membrane into contact with the syringe in <10 msec. The bottom of the holder is connected to a vacuum pump. Fusion 5 membranes (GE Healthcare Life Sciences) were cut into 22 mm circles using a Silhouette Cameo 3 Desktop craft cutter. Anti-bacteriophage M13 polyclonal antibodies (Novus Biological, NB100-1633) or NeutrAvidin (ThermoFisher Scientific) at varying concentrations were immobilized on Fusion 5 membranes (GE Healthcare Life Sciences) in a 50 mM sodium acetate (pH 3.6) solution and allowed to air dry for 24 h. Alexa 555-labeled or biotinylated Alexa 555-labeled phage (10^{8} pfu/mL) was loaded into a syringe driven by a stepper motor (BioLogic). The rapid filtration apparatus was updated with an Arduino Nano microcontroller and controlled by a custom graphical user interface (GUI) LabVIEW program (National Instruments) (code can be accessed

through GitHub: https://github.com/willsonlab/rapidfiltration). The LabVIEW program takes inputs as flow rate (mL/sec) and duration (msec) and then maps the desired flow rate (0.5 to 9 mL/sec) to the calibrated pulse frequency for the stepper motor driver (40 to 2268 Hz). The pulse frequency and duration parameters are sent from the LabVIEW program to the microcontroller via serial communication. Upon activation, the microcontroller activates the solenoid actuator to bring the membrane into contact with the syringe and sends square pulse outputs to the syringe stepper motor to initiate flow. The liquid passing through the membrane is removed by vacuum. After a specified duration, the microcontroller simultaneously stops syringe-driving pulses and deactivates the solenoid actuator. By spring action, the membrane is then separated from the syringe creating an air gap between them and preventing further liquid contact.

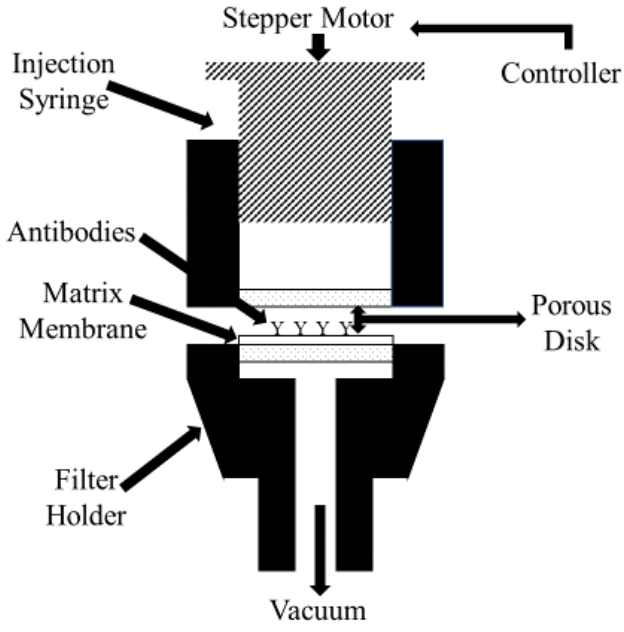

Figure 6: *Rapid Filtration Apparatus.*

The stepper motor is initiated by an Adruino Nano microcontroller controlled by a LabVIEW GUI, and in combination with a solenoid activation, brings the movable filter holder to come into contact with the syringe, thereby initiating contact between the two stainless steel porous disks and liquid being able to flow.

Membrane Phage Extraction

Rapid filtration experiments were performed using Alexa 555-labeled phage (10^8 pfu/mL), and the bound phage was first measured in situ, the captured phage in a Fusion 5 membrane, and was then recovered. Fusion 5 was spotted with the membranes' water absorptive capacity volume (152 µL/380 mm^2) of anti-M13 antibodies (4.3 µg/mL) in 50 mM sodium acetate (pH 3.6), for antibody immobilization through electrostatic adsorption. For recovery of bound phage, the Fusion 5 membrane was soaked in 500 µL of 7 M urea and vortexed for 1 hour, followed by centrifugation (10 minutes, 16,000 *x g*). Initial experiments used a 6 mm biopsy punch to puncture the membrane for fluorescence recovery, before switching to using the whole membrane. The supernatant was transferred to a 96-well plate (Greiner Microlon) and read using a fluorescence plate reader (Infinite M200 Pro, TECAN; Ex: 525 nm/Ex: 568 nm). As a control, additional cycles of urea recoveries and centrifugation of the membrane in 500 µL of 7 M urea were performed to confirm complete recovery of Alexa 555-labeled phage.

Protein Assay of Membrane Immobilized Antibodies

Circular disks (10 mm) of Fusion 5 membrane were placed in Eppendorf tubes containing 200 µL of 0-40 µg/mL of anti-M13 antibody in 50 mM sodium acetate, pH

3.6, and incubated for 1 hour. Fusion 5 disks were removed and put into a second Eppendorf tube, and the supernatant antibody solutions were transferred into a 96 well plate. All three samples (original antibody solution, antibody-loaded dish, and the supernatant containing uncaptured antibodies) were assayed by micro bicinchoninic acid (Thermo Fisher Scientific, #23235) using anti-M13 antibodies as standards. Samples were incubated at 37℃ for 2 hours and then allowed to cool to room temperature. The absorbance was read at 562 nm.

Results and Discussion

Rapid Filtration Apparatus Calibration

The flow of the rapid filtration apparatus system can be adjusted from 0.50 mL/sec to 9 mL/sec for varying durations (minimum of 10 msec). The dead time for the motorized syringe coming in contact with the stainless-steel porous support is 10 msec. Updating the rapid filtration apparatus with a new microcontroller and LabVIEW software required the flow rates and duration to be re-calibrated with distilled water measured gravimetrically. Flow rate durations accuracy was confirmed by the linear relationship between the dispensed and calculated volumes with an R-squared value of 0.99 (Figure 7A).

The absorptive capacity of the Fusion 5 membrane was calculated to determine antibody loading volumes. The water capacity for the Fusion 5 membrane with a diameter of 22 mm was 152 µL. The capacity was tested with red color food dye (McCormick) with a volume above and below the capacity to determine the effects of membrane drying test for and noticeable coffee-ring effects. These effects originate by capillary flow induced by differential evaporation rates and can cause an increased

antibody concentration at the edge of the membrane, affecting the uniformity of antibody immobilization. For porous matrices, if liquid infiltration is faster than evaporation and particle motion, and the coffee-ring is suppressed[101]. The pore size of the membrane will affect the presence of a coffee ring, and if a pore size is small, as with Fusion 5, capillary flow is slow and thus reduces coffee ring formation[102]. The coffee ring line will be significantly reduced due to the antibody being suspended in a sodium acetate solution that will electrostatically interact with the silica fibers of Fusion 5, allowing antibody immobilization uniformly across the membrane.

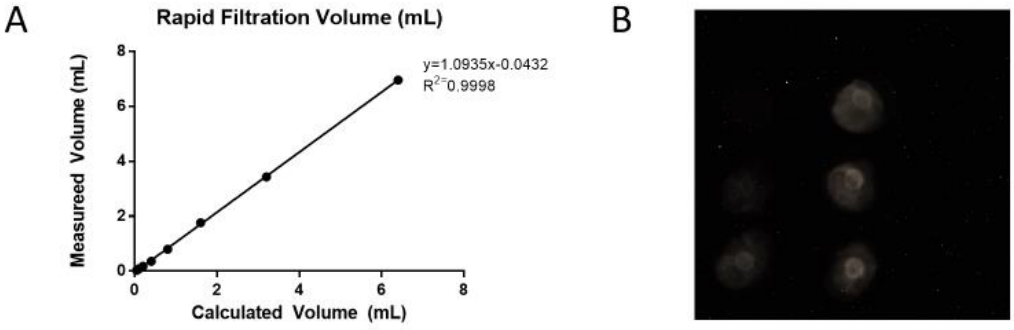

Figure 7: *Calibration of the Rapid Filtration Apparatus. A) Calibration curve based on measured liquid and calculated volume. B) Chemiluminescence imaging of captured phage.*

The liquid dispensed by the motorized syringe was measured on an analytical balance and was plotted as a function of the calculated volume (flow rate x duration) to create a calibration curve (Fig. 7A). A linear fit was performed with an R-squared value of 0.9998. Chemiluminescence measurements of captured phage. 50 µL of anti-M13 antibody in 50 mM sodium acetate, pH 3.6 was spotted on the membrane, and

disks were allowed to air dry for 24 hr. Biotinylated M13 bacteriophage (10^8 pfu/mL) passed through the syringe at 3 mL/sec for 0, 50, 100, 200, 400 and 800 msec (top left to right and rastering by raw). This was followed by flowing 1 ng/mL of streptavidin-HRP and three washes of 0.1% TWEEN at 3 mL/sec for 100 msec. 152 µL of luminol was spotted on the membrane. The image was taken by a camera (Photometrics CoolSNAP K4) with an exposure time of 2 seconds (Fig. 7B).

Several methods of measuring the amount of phage captured were tested: chemiluminescence imaging, in situ fluorescence, and recovery of bound phage, followed by measurements in solution. To measure captured phage through chemiluminescence imaging, biotinylated M13 phage was passed through disks immobilized with anti-M13 antibodies followed by streptavidin-horseradish peroxidase (HRP). The chemiluminescence reaction was confirmed by the chemiluminescence reaction catalyzed by HRP with an advanced chemiluminescent luminol substrate, FemtoGlow (Michigan Diagnostics, SHRPM 21004) by spotting 152 µL of FemtoGlow on the disk and was imaged by Photometrics COOLSNAP K4 camera, with an exposure time of 2 seconds (Figure 7B). This methodology was not chosen to measure the capture of M13 in the porous matrix due to the background chemiluminescence (membrane area without anti-M13 antibody) interfering with capture signal.

In Situ Fluorescent Measurements of Alexa 555-labeled Phage

M13 bacteriophage labeled with Alexa 555 fluorescence was measured in solution and on Fusion 5 membranes by a plate reader. A fluorescence peak height

was observed at 568 nm. Dried Fusion 5 membranes exhibited a higher background fluorescence (~1,500-200 fluorescence units) when compared to wet membranes. During the formation of Fusion 5 membranes, proprietary binders are used that can cause the membranes to exhibit fluorescence when the silica fibers are not wet.

Alexa 555 labeled-phage was loaded into the rapid filtration syringe and then flowed through a Fusion 5 membrane with immobilized anti-M13 antibodies. The membranes were sampled with 6 mm biopsy punches at various locations and transferred to a 96 well plate. The fluorescence intensity at 568 nm upon excitation at 525 nm in the TECAN plate reader was evaluated using the peak height. Varying flow rates and times were used to assess the capture of Alexa 555-labeled phage to anti-M13 antibodies (Fig. 8A). With increasing flow rates, the fluorescence intensity also increases, such that there is a filtering effect, in that increasing amounts of Alexa 555-labeled phage passing through the membrane allows more to get caught. Peak heights were also obtained for membranes without anti-M13 antibodies and served as the fluorescence background (Fig. 8B). When comparing flow rates, the fluorescence saturation is faster at high flow rates, 8 mL/sec, compared to lower flow rates, 1 mL/sec. At 8 mL/sec, the residence time in the 370 μm thick membrane is 20 msec. The membranes' surface capacity in terms of fluorescence was the capture of Alexa 555-labeled phage on immobilized anti-M13 antibodies with the background membrane fluorescence subtracted as a function of the volume, flow rate x time (Fig. 8C).

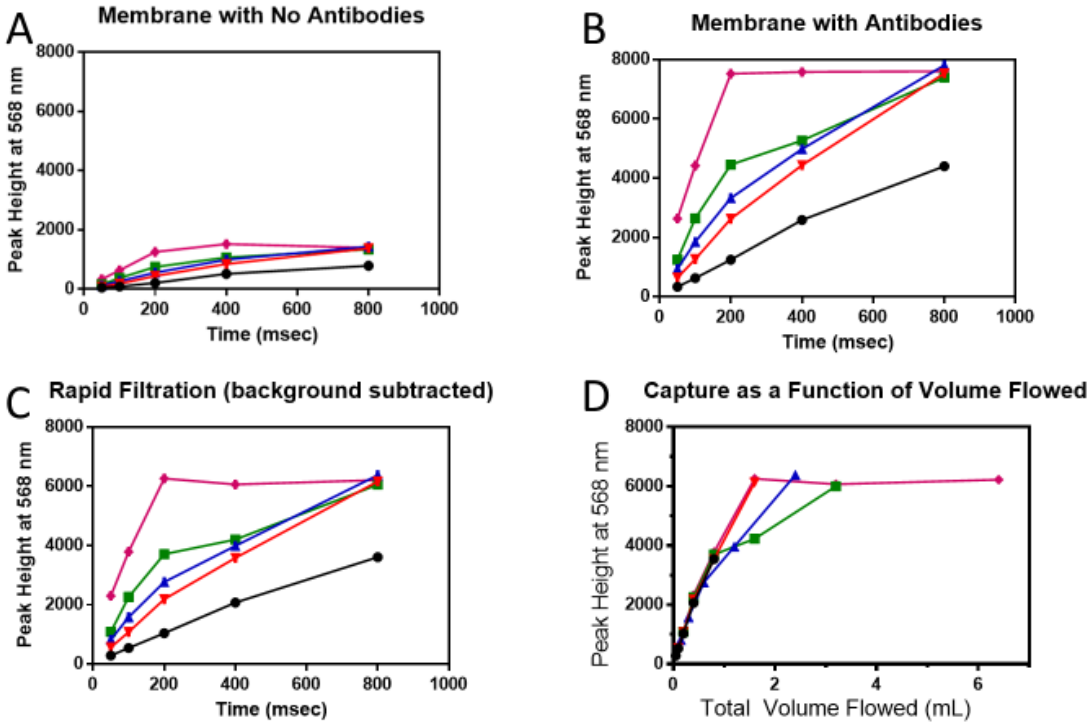

Figure 8: *Capture of Alexa 555-labeled phage. A) Membrane without antibodies. B) Membrane with antibodies. C). Capture on the membrane with antibodies with membrane without antibodies subtracted. D). Capture as a function of volume flowed.*

Capture of Alexa 555 labeled-phage (10^8 pfu/mL) on Fusion 5 membranes with immobilized anti-M13 antibodies (4.3 µg/mL) with varying flow rates: ●, 1 mL/sec, ▼, 2 mL/sec, ▲, 3 mL/sec, ■, 4 mL/sec, ♦, 8 mL/sec. Membrane with no antibodies (50 mM sodium acetate-pH 3.6) and Alexa 555-labeled phage in PBS was passed through the system (Fig. 8A). Membrane with immobilized anti-M13 (4.3 µg/mL) antibodies and Alexa 555-labeled phage (10^8 pfu/mL) passed at selected flow rates and time through the system (Fig. 8B). Alexa 555-labeled phage capture in Fusion 5 with the data from graph A subtracted for background noise (Fig. 8C). Alexa 555-labeled phage captured as a function of volume flowed based on the flow rate and volume passed through Fusion 5 (Fig 8D).

As the initial front of the liquid dispensed from the syringe comes in contact with the porous membrane, the liquid wicks radially and flows further through the membrane at faster flow rates (8 mL/sec) and longer times (800 msec). At these flow rates and times, M13 may get displaced compared to slower rates (1 mL/sec) and times (100 msec) where the phage is binding to its recognition elements and being caught in the top part of the membrane. While flow rates would affect the binding of Alexa 555-labeled phage, the rapid filtration apparatus yields similar fluorescence values when comparing the total volume passed through the membrane, indicating binding is very fast compared to the flow rate (Fig. 8D). However, only the fluorescence on the top of the membrane was able to be measured in the plate reader. The total fluorescence of Alexa 555-labeled phage through the depth of the membrane cannot be accurately read. If the membrane is flipped upside down, the fluorescence values differ. Therefore, there is a fluorescence gradient through the 370 μm membrane thickness, depending on the flow rate and time.

Filamentous M13 is highly anisotropic with a length of approximately 900 nm and a width of approximately 6.6 nm. Due to its aspect ratio, which is advantageous for chemical modification and improved readout in LFAs, it has limitations in porous membranes. Fusion 5 matrix has a pore diameter of 11 μm and an average fiber diameter of D=4.35 ± 1.90 μm allowing phage to interact with the fibers and possibly be caught in the pores of the membrane[89]. When M13 is run on Fusion 5 membranes for LFAs multiple washing steps with 0.1% TWEEN, a polysorbate nonionic surfactant, are needed. Flowing surfactant after Alexa 555-labeled phage is passed

through the rapid filtration apparatus will alter its capture. Due to these possibilities, the total fluorescence of M13 phage embedded within the Fusion 5 membrane cannot be accurately measured. To measure the total Alexa 555-labeled phage captured within Fusion 5, index matching was used to read the total fluorescence. With a high refractive index of 1.457 for Fusion 5, a viscous glycerol solution did not allow for a total fluorescence reading[103]. Index matching is not possible for Fusion 5 due to its composition properties of silica fibers and proprietary binders.

Measurement of Phage by Recovery from the Membrane

To measure the total fluorescence recovery of the membrane in varying liquids to read the total fluorescence. A variety of solutions did not fully extract the captured Alexa 555-labeled phage (PBS and H_2O), while other solutions caused a high background fluorescence ranging from ~1,500-5,000 fluorescence units at 568 nm. (1 M HCl, 7 M guanidine hydrochloride). 7 M urea was found to give the most complete recovery of fluorescence from the porous membrane. By soaking the membrane in 7 M urea, Fusion 5 was disintegrated into fibers, allowing the phage to be released. This disintegration was not observed with the other recovery solutions tested. When Alexa 555-labeled phage is vortexed in urea, no significant loss of fluorescence was detected. The membrane was soaked in 500 μL of 7 M urea and vortexed for 1 hour. After centrifugation, the supernatant fluorescence was read. During recovery to ensure the fluorescence from Alexa 555-labeled phage was accurately measured, multiple factors were tested, such as background membrane fluorescence, if vortexing affects the fluorescence of Alexa 555-labeled phage and the Eppendorf tube fluorescence

(~500 fluorescence units at 568 nm). After establishing these factors have minimal effects on the total fluorescence, membranes immobilized with and without anti-M13 antibodies were spotted with Alexa 555-labeled phage and then soaked for recovery of fluorescence (Fig 9).

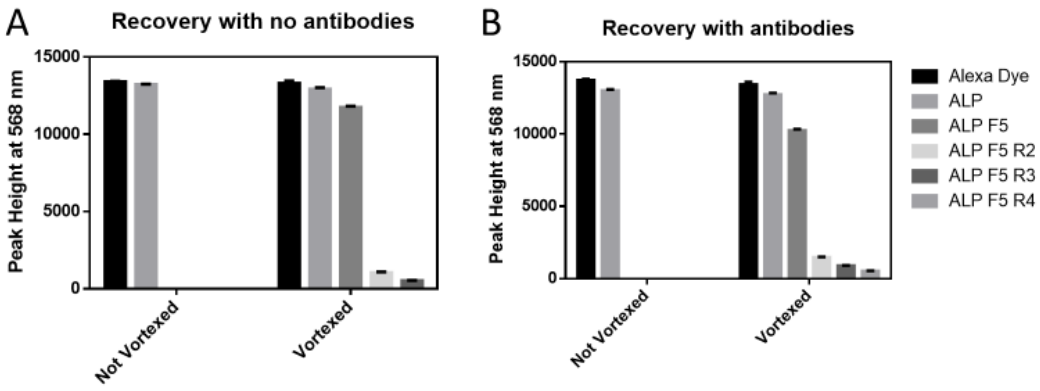

Figure 9: *Measuring Fluorescence of Alexa 555-labeled phage A) Recovery on membranes without antibodies. B) Recovery on membranes with anitbodies.*

Alexa 555-labeled phage (10^8 pfu/mL) was incubated in 7 M urea for 1 hour in vortexed and non-vortexed conditions (Fig 9A). Recovery of Alexa 555-labeled phage (ALP) from the membrane with no antibodies. Free Alexa dye and Alexa 555-labeled phage were compared in non and vortexed conditions. Alexa 555-labeled phage (10^8 pfu/mL) was spotted onto Fusion 5 (F5) 22 mm disks and then dried for 24 hours. The membrane was vortexed in 500 µL of 7 M urea for 1 hour and centrifuged (10 min, 16,000 x g). The supernatant was collected, and its emission was read at 568 nm (ALP F5). Further recoveries (R2, R3, R4) of the membrane in 500 µL of 7 M urea with

vortexing (1 h) and centrifugation were performed. Each supernatant was then read at 568 nm.**).** Recovery of Alexa 555-labeled phage from the membrane with anti-M13 antibodies (150 µL of 4.3 µg/mL per 380 mm^2) (Fig. 9B).

In comparing the total fluorescence at a peak height of 568 nm between unconjugated Alexa dye and Alexa 555-labeled phage, there is a loss of fluorescence (8%) as this is most likely due to Alexa 555 coupling (Fig 9A and 9B). To obtain >95% of the total fluorescence, an additional recovery period for membranes immobilized with anti-M13 antibodies is needed (Fig. 9B). With additional recoveries, the Fusion 5 membrane disintegrates, becoming a fibrous clump. Based on this data and creating baseline curves, Alexa 555-labeled phage (10^8 pfu/mL) was passed through Fusion 5 membranes with anti-M13 antibodies (4.3 µg/mL) and membranes without antibodies. Various flow rates were performed: ●, 1 mL/sec, ▼, 2 mL/sec, ▲, 3 mL/sec, ■, 4 mL/sec, ♦, 8 mL/sec. The membrane was soaked in 7 M urea for 1 hour, vortexed, centrifuged, four times for complete recovery of phage. Each time the supernatant was collected, 568 nm peak heights summed. The fluorescence captured on membranes without antibodies was subtracted from membranes with antibodies. At higher flow rates (4 mL/sec and 8 mL/sec), a higher total fluorescence is exhibited (Fig. 10). However, for an 8 mL/sec flow rate at 200 msec and longer times, the fluorescence levels off, indicating that capture of Alexa 555-labeled phage is reduced. Additionally, this would indicate that faster flower rates assist in the binding of M13 to its recognition element, while at slower rates, longer times are needed for capture.

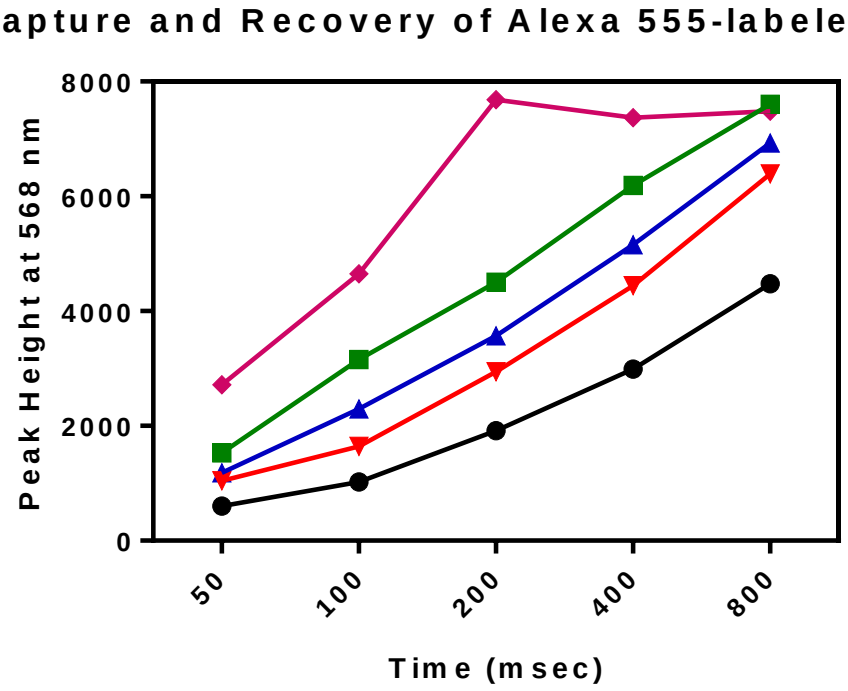

Figure 10: *Rapid Filtration Recovery*

To determine the capture of Alexa 555-labeled phage the percent capture was calculated based on the liquid fluorescence recovery by the offered fluorescence (Fig 11 A and B). Alexa 555-labeled phage (10^8 pfu/mL) was passed through the membrane immobilized with anti-M13 antibodies (4.3 µg/mL) The fluorescence of Alexa 555-labeled phage in solution was measured before it was passed through the rapid filtration apparatus. The liquid fluorescence of Alexa 555-labeled phage after being passed through the membrane was recovered at varying flow rates: ●, 1 mL/sec, ▼, 2 mL/sec, ▲, 3 mL/sec, ■, 4 mL/sec, ♦, 8 mL/sec. Percent not captured was calculated based on the fluorescence before passed through rapid filtration apparatus by the fluorescence captured by the vacuum. These values were subtracted from one to obtain percent captured.

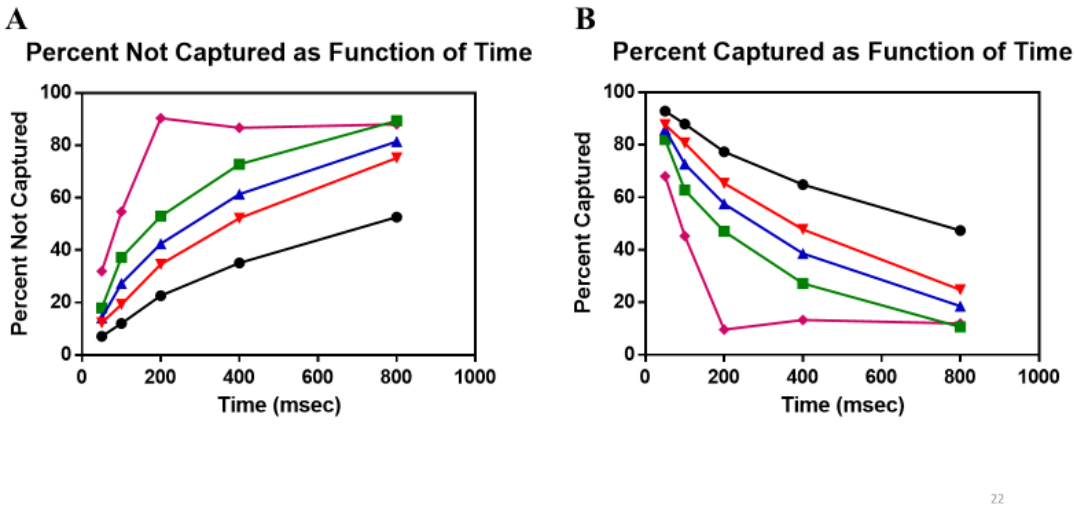

Figure 11: *Percent Capture of Alexa 555-labeled phage. A) Percent not captured based on liquid fluorescence readings. B) Percent captured based on not captured subtracted from one.*

There is a greater percent captured at faster flow rates and reaches a threshold in the Fusion 5 membrane. There are possible ways for reduced capture at longer flow times from the antibody binding sites fully occupied, steric hinderance of M13 phage blocking other M13 from antibody capture, or the immobilized antibody is not properly oriented for capturing phage.

Micro BCA Quantification of Membrane Immobilized Antibodies

To calculate the amount of antibody immobilized on the Fusion 5 membrane, a micro BCA assay was performed in a depletion format. An initial antibody solution was measured the contacted with the membrane in an Eppendorf tube, and the protein remaining unbound in the supernatant was measured. To measure if any protein was attaching to its walls, the Eppendorf tube was also analyzed. For the BCA assay, the

absorbance was measured at 562 nm, with the lowest concentration measured at 2.0 µg/mL and an anti-M13 standard curve. After protein concentrations were calculated and compared between the initial and post soak solutions, the Eppendorf tube, and the Fusion 5 membrane, the amount of protein per membrane (78.54 mm^2) varied from 0.73 ug to 3.7 ug based on anti-M13 offered (Fig. 12).

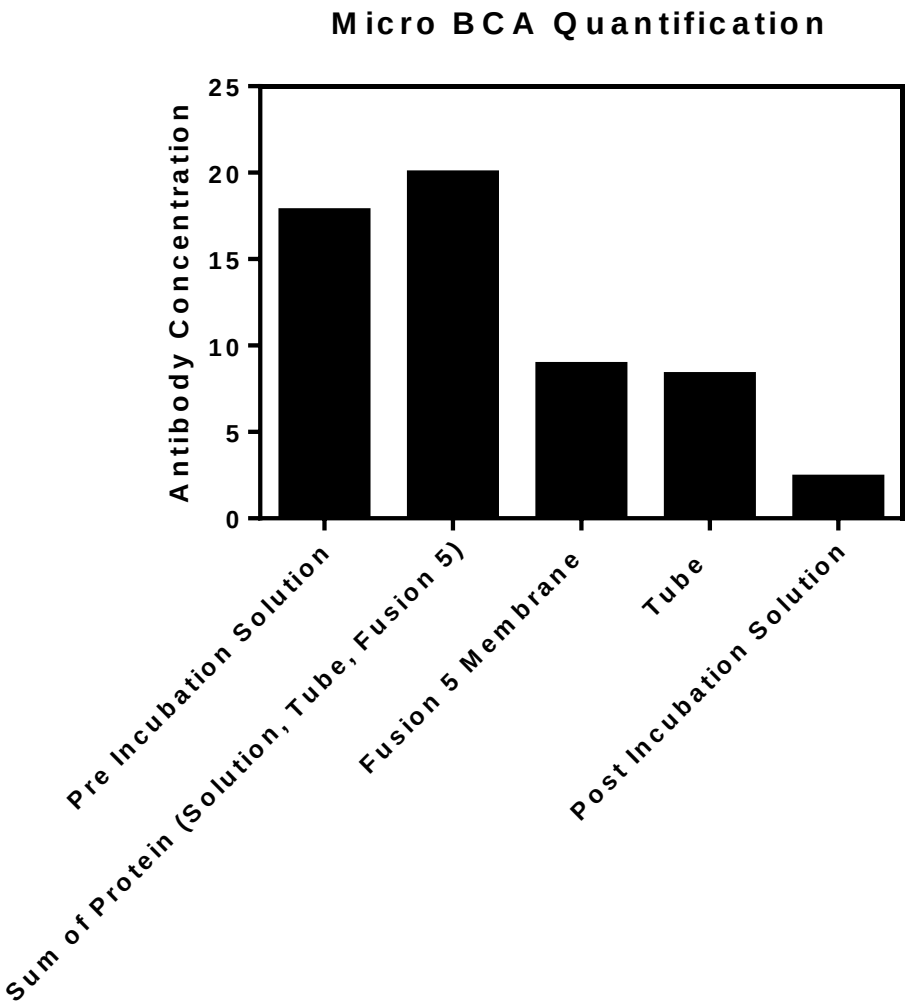

Figure 12: *Micro BCA Assay Quantification of Membrane Immobilized Antibodies*

Fusion 5 membranes were punctured (10 mm) and incubated in an anti-M13 antibody (17.2 µg/mL) 50 mM sodium acetate solution (pH 3.6) for 1 hour. Membranes were removed and put into another Eppendorf tube. The post incubation solution, the Fusion 5 membrane, and the Eppendorf tube were incubated with 150 µL of the BCA microassay master mix for 2 hours at 37 °C and read at 562 nm. Antibody concentrations were calculated based on an anti-M13 antibody standard curve.

Initial phage capture experiments were performed with a low concentration of anti-M13 antibody (4.3 µg/mL) contacting the membrane, immobilizing at an amount of 0.7 µg/78.5 mm^2 (8.9 ng/mm^2). The protein per area on a 3 mm wide lateral flow strip with a 0.3 µg antibody loading on a 0.75 mm line width is 130 ng/mm^2. Thus, initial capture experiments with the rapid filtration apparatus and subsequent recovery protocols were at a lower antibody immobilization per membrane area. To more closely match LFA strip antibody loading, the membrane concentration for rapid filtration analysis was increased from 4.3 µg/mL to 17.2 µg/mL to more closely match that within a typical lateral flow strip. Varying concentrations of the recognition element on the porous matrix will affect the capture of the reporter particle or analyte[104,105]. Alexa 555-labeled phage was passed through membrane at varying flow rates and recovered using 7 M urea. At a higher antibody loading, the total fluorescence within the membrane with the background-subtracted is higher compared to a lower antibody loading at the same volumes (Fig. 13).

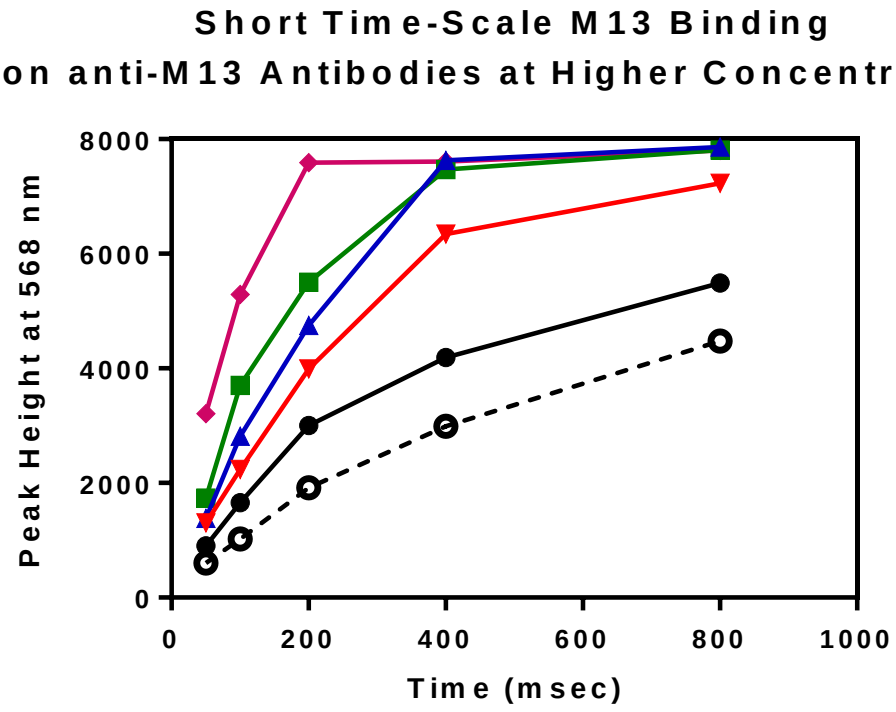

Figure 13: *Rapid Filtration Recovery on Fusion 5 Membranes at Higher Antibody Concentrations.*

Rapid Filtration Recovery on Fusion 5 membranes immobilized with anti-M13 antibodies at 2.9 µg/mm^2. 150 µL of anti-M13 antibody (17.2 µg/mL) was immobilized on the Fusion 5 membrane and was allowed to air-dry for 24 hours. Two anti-M13 loadings were compared, 4.3 µg/mL and 17.2 µg/mL. For 4.3 µg/mL, only one flow rate (**O**, 1 mL/sec) is graphed with the higher antibody loading. For the 17.2 µg/mL antibody loading various flow rates of Alexa 555-labeled phage (10^8 pfu/mL) were passed through the rapid filtration at varying flow rates: ●, 1 mL/sec, ▼, 2 mL/sec, ▲, 3 mL/sec, ■, 4 mL/sec, ♦, 8 mL/sec. Recovery protocols were performed, as previously explained, with vortexing and centrifugation.

To determine the percent, capture the fluorescence of Alexa 555-labeled phage in solution was measured before being passed through the rapid filtration apparatus (Fig. 14). The liquid fluorescence of Alexa 555-labeled phage after being passed through the membrane was recovered **O**, indicates 1 mL/sec at 4.3 µg/mL anti-M13 loading. Loadings for 17.2 µg/mL at varying flow rates: ●, 1 mL/sec, ▼, 2 mL/sec, ▲, 3 mL/sec, ■, 4 mL/sec, ♦, 8 mL/sec. Percent not captured was calculated based on the fluorescence before being passed through the rapid filtration apparatus by the fluorescence captured by the vacuum. These values were subtracted from one to obtain percent captured.

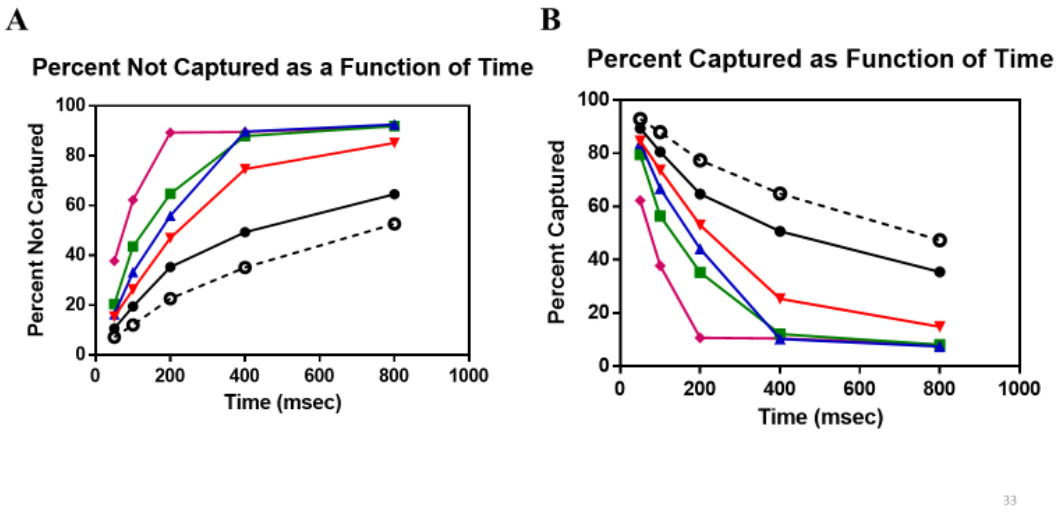

Figure 14: *Effects of Antibody Loading on Capture Efficiency. A) Percent not captured based on liquid fluorescence readings. B) Percent captured based on not captured subtracted from one.*

In comparing percent captured, at 1 mL/sec at different antibody concentrations, there is a higher percent capture at a higher loading of immobilized antibody (Fig 14A and B). Thus, with a higher antibody loading, more M13 is able to

bind to its recognition element. The same trend is also observed with faster flower rates, of M13 binding to its recognition element. With a higher concentration of anti-M13 antibody and based on the fluorescence intensity peaks, more capture sites allow for faster binding. At low flow rates, 1 mL/sec, capture is slower.

The Capture of Biotinylated M13 Phage on NeutrAvidin

We have previously reported that M13 phage captured by anti-M13 antibodies exhibit differences in the distribution of orientational binding modes when compared to capture by NeutrAvidin for functionalized LFA membranes[89]. For use in the rapid filtration apparatus, Fusion 5 membranes were loaded with NeutrAvidin (4.3 µg/mL) in 50 mM sodium acetate, pH 3.6, at 645 ng/380 mm^2. Initial experiments started with dilute concentrations of NeutrAvidin similar to the capture studies of M13 phage to anti-M13 antibody at a flow rate of 3 mL/sec. The capture of biotinylated M13 phage to NeutrAvidin at a concentration of 4.3 µg/mL was not detectable at 50 to 200 msec due to the membranes' background fluorescence without immobilized NeutrAvidin. As the time of flow increases from 50 to 800 msec, capture is more visible towards the longer time points. There was a weak dependence on NeutrAvidin loading as capture goes to completion, so for further capture characterization, the NeutrAvidin loading on the membrane was increased to determine a concentration for the binding to biotinylated M13 phage for rapid filtration analysis. With increased loadings of NeutrAvidin on the Fusion 5 membrane, the capture of biotinylated Alexa 555-labeled phage increases at the time points measured (Fig. 15). This further indicates that a higher loading of NeutrAvidin is needed to measure the capture of biotinylated Alexa

555-labeled phage on the rapid filtration apparatus. Identically-treated antibody-free membrane exhibited a background signal, <1,000.

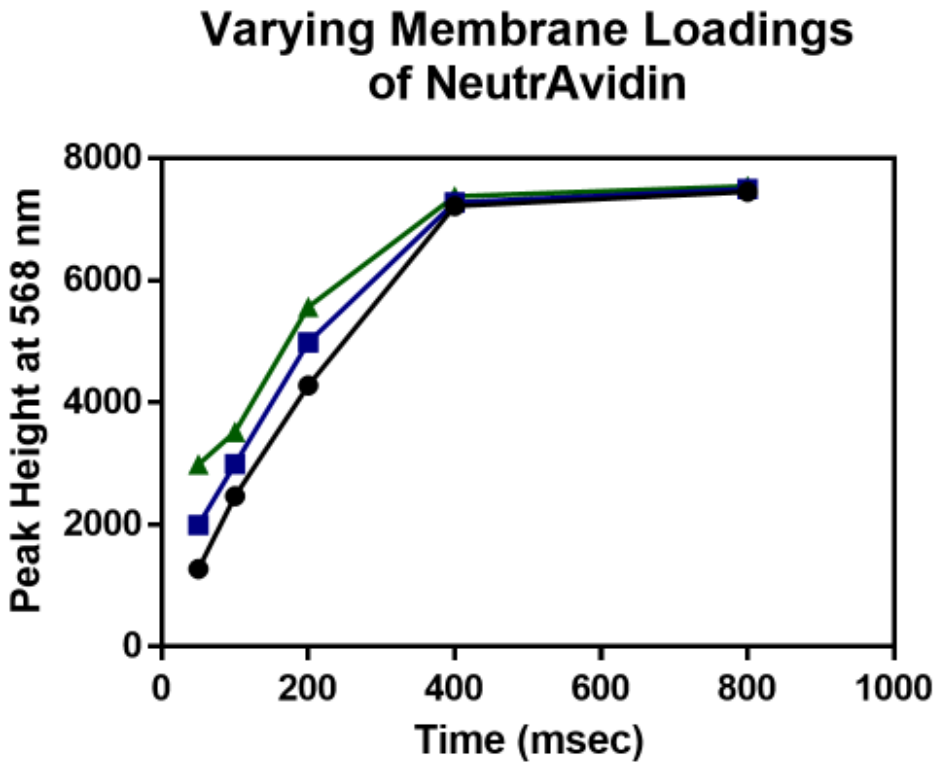

Figure 15: *Membrane Loadings of NeutrAvidin*

Varied concentrations of NeutrAvidin, ●, 10 µg/mL, ■, 20 µg/mL, and ▲ ,50 µg/mL was immobilized on Fusion 5 membranes in 50 mM sodium acetate (pH 3.6) solutions. Biotinylated Alexa 555-labeled phage (10^8 pfu/mL) was passed through the rapid filtration apparatus at 3 mL/sec. The membrane was punched out with 6 mm biopsy punches, and the membrane was read at 568 nm. Fluorescence readings from membranes with no NeutrAvidin were subtracted.

The rate of capture is higher with increased NeutrAvidin, but the fluorescence plateau is the same across the varied NeutrAvidin loadings indicating that capture is faster than the flow rate Also, due to M13 phage being biotinylated, the amount of Alexa labeled dye per phage differs from the amount of dye per phage without any biotinylation. Additionally, the orientational binding modes of phage to anti-M13 antibody or NeutrAvidin differ from side to tip binding. While the affinity of biotin for avidin is higher, tip binding by the capture of NeutrAvidin indicates a higher loading of the recognition element, but further studies are needed to address these issues.

Conclusions

In LFAs, the interaction time between a reporter particle and its immobilized recognition element where binding occurs is on the order of milliseconds. Various factors may affect this interaction, such as the geometry of the reporter, the buffer solution, the biological sample, and the properties of the porous matrix[106–108]. While LFAs vary in these factors, we have demonstrated the use of M13 bacteriophage reporters leads to an increased sensitivity of the assay[49]. The binding of bacteriophage to recognition elements on porous membranes has not been fully characterized to understand the assays' increased sensitivity. By adjusting the fluid flow rate, especially decreasing the rate, analytical sensitivity has been improved[109]. To further understand the interaction of M13 with its recognition elements at a short-time scale, rapid filtration will yield insights for further characterization. Previously, studies indicated a faster flow rate is better for the capture of M13 phage to anti-M13 antibodies[89]. The rapid filtration apparatus is versatile, allowing the use of other

reporters or analytes to be analyzed. As a novel technique, the rapid filtration apparatus can provide insights into binding kinetics by varying the analyte and capture agents. We established a rapid filtration assay that can precisely dispense liquid volumes with the ability to test the solution on the porous membrane. Additionally, the rapid filtration apparatus uses a porous membrane in which proteins or analytes are immobilized on porous substrates. These studies will characterize the capture of reporters for LFA and vertical flow. Additionally, the pore dimensions of the stainless mesh for the rapid filtration apparatus are on the order of 100 μm, so the capture of reporter particles of varying dimensions can be used in the rapid filtration apparatus.

Rapid filtration allows the measurement of adsorption in membranes on the sub-second time-scale. It is anticipated the measurements can help understand the remarkable sensitivity of the phage-based lateral-flow test. By varying the flow rate and timing, the capture of M13 bacteriophage at low and high antibody loading rates can be understood. This will allow the optimization of lateral and vertical flow conditions for a higher degree of capture and increased sensitivity. The insights to characterize capture at short-time scales below one second is crucial for the understanding of antibody purification, chromatographic and membrane adsorption, and membrane-based assays and medical diagnostics.

CHAPTER 3: LYOPHILIZATION OF BACTERIOPHAGE LATERAL FLOW ASSAYS

Introduction

Point-of-care (POC) testing allows for patient diagnostics away from central laboratories, in the physician's office, rural areas, ambulances, and at home. It allows for the rapid detection of analytes near the patient, which facilitates better disease diagnosis, monitoring, and management. The global POC testing market is expected to grow in the U.S. from $23.2 billion in 2016 to $40 billion in 2021 at a compound annual growth rate (CAGR) of 10%[14,15]. POC diagnostics are affordable, rapid, and offer a degree of sensitivity and specificity that is crucial for testing in resource-limited settings. They enable quick medical decisions and may provide earlier detection, leading to improved health outcomes for patients by allowing early treatment.

A major class of POC diagnostics is lateral flow immunoassays (LFAs), in which reporter particles are transported to binding sites by capillary wicking in a porous membrane. LFAs most often employ antibodies attached to detectable reporters as recognition elements. LFAs have employed various reporters—colloidal gold, colored latex particles, phosphors, magnetic particles, carbon nanotubes, and virus particles—that have demonstrated a sensitivity applicable for the desired immunoassay[44,49–52]. Readouts for LFAs vary based on the reporter particle and external devices employed, with readouts ranging from colorimetric, magnetic, and light-based to spectral based readouts[52,57,110,111]. The performance of LFAs can be improved by adjusting the, including the reporter particle, fluid velocity, reagent concentration, and

the membrane type[80,89]. Increasing the quantitative nature and analytical sensitivity of LFAs would expand their usefulness across a variety of fields.

While various reporter particles have been implemented into LFAs, the choice of the particle and the corresponding detection method directly affect the performance of the assay. Depending on the reporter particle, chemical modifications can be difficult, and the choice of reporter particle can lead to a compromise between ease of chemical modifications and sensitivity. One approach to addressing these issues is the use of bacteriophage as LFA reporters, which we recently introduced[49]**.** Functionalized viral nanoparticles have been explored in recent years for use as reporters in immunoassays, resulting in higher sensitivity and low limits of detection[97,112,113]. Filamentous M13 bacteriophage, in particular, has been modified with recognition and reporter elements, and successfully used for diagnostics, medical, and imaging purposes[73–75]. The high surface-area-to-volume ratio of an M13 phage is advantageous in lateral flow and assures its neutral buoyancy. M13 phage is ~900 nm in length and ~6 nm in width and can be genetically modified to different aspect ratios[114,115]. The surface of a bacteriophage consists of multiple copies of identical coat proteins, which allows for its chemical modification and wide adaptability as a reporter for LFAs. Others have demonstrated a variety of chemistries have been adapted for M13 phage to perform a wide range of chemical linkages and functional groups[116,117]. Previously, we introduced engineered M13 phage particles as reporters in lateral flow assays that resulted in a 100-fold greater sensitivity in the detection of human chorionic

gonadotrophin (hCG) when compared to conventional gold nanoparticles in pregnancy-based tests[49,50].

Several novel laboratory-developed LFAs have demonstrated improved limits of detection but suffer from future test optimization for their widespread implementation. Long-term stability under different environmental conditions, device portability, and maintaining high sensitivity are unique advantages related to LFAs. Translational of these lab advantages of phage LFAs to practical diagnostics requires the development of storage-stable forms and compatibility with blood samples. Before the commercialization of LFA strips, several aspects of the strip have to be carefully examined from the optimization of the assay steps, material properties, storage stability, and the read-out result[40]. Each reporter particle used in an LFA requires optimization and subsequent testing to ensure the test's sensitivity is maintained across the shelf-life of an LFA. Furthermore, LFAs have shown great promise in the laboratory but have failed further assay development, since the interaction of various reporter particles and signal generation has cross-reacted in clinically relevant samples[118]. To further affirm M13 phage use as a reporter particle in LFA we set out to optimize the strip in terms of the membrane, long-term storage of reporter particle within the conjugate release pad, and test the sensitivity of M13 phage in blood to determine if differences exist over a one month accelerated stability period.

Materials and Methods

Culture and Titering of M13 Bacteriophage

M13 phage displaying the AviTag, a substrate peptide on the p3 tail protein, was a gift from Dr. Brian Kay (The University of Illinois at Chicago). Culture and

titering of M13 phage were performed as described previously[97]. AviTag-M13 was pre-mixed with *Escherichia coli* TG1 culture for two hours at 37℃ and was transferred to 2x yeast extract and tryptone (2 x YT) broth medium for overnight growth at 37℃. Bacteria were separated from the lysate by centrifugation (30 min, 3,200 *x g*) followed by filtration through a 0.45 μm filter (Corning, #430512). Phage were then precipitated using PEG/NaCl as previously described[99]. Phage titers were determined on X-Gal/IPTG plates as described[98].

Preparation of LFA Strips

0.5 μL of rabbit polyclonal anti-M13 IgG antibody (4.3 mg/mL) (Novus Biologicals, Littleton, CO) diluted in 50 mM sodium acetate buffer (pH 3.6) was used to spot the test line. CF5 membrane (GE Healthcare, Piscataway, NJ) was used as the absorbent pad (18 mm), silica-fiber Fusion 5 membrane (GE Healthcare, Piscataway, NJ) was used as the sample pad (12 mm), and the membrane (22 mm), and Standard 14 (8 mm) was used as the conjugate release pad. Nitrocellulose FF 80 HP (GE Healthcare, Piscataway, NJ) was also tested as a conjugate release pad. The lateral flow strip was assembled using a manual laminator (Shanghai Kinbio Tech Co.) with a 2 mm overlap for each adjacent component. Strip components were assembled on a plastic backing card (DCN Diagnostics, #MIBA-020) and cut to a width of 3 mm using a guillotine cutter (Shanghai Kinbio Tech Co, Automatic Cutter, ZQ2000) and stored in a desiccant box at 25% relative humidity.

Lyophilization

The strips were cooled for 1 hour in a -80°C freezer and then transferred on an ice block to a lyophilization chamber (LabConco, -56°C, 0.090 Pa) for 16 hours. Concurrently, a control set of strips were air-dried for 17 hours at ambient temperature on a lab bench.

Lateral Flow Assay with Phage Reporters

Strips were washed two times with 20 μL washing buffer (1% PBS, 0.5 % TWEEN-20, 0.5% BSA). 20 μL of 10^{10} M13 phage/mL in PBS was added, followed by three washes of 20 μL of washing buffer. For the detection of human chorionic gonadotrophin (hCG), the M13 anti-hCG conjugate was stored in the conjugate release pad. 20 μL of (hCG) diluted in PBS was added to strip first followed by three washes of 20 μL washing buffer. For M13 and hCG detection, 20 μL of anti-M13 HRP diluted in 1% PBS, 0.5 % TWEEN-20, 0.5% BSA was added. Strips were then washed five times with 20 μL of washing buffer. Signals were visualized by spotting 5 μL of blotting 3,3',5,5'-Tetramethylbenzidine (TMB) on the membrane test spot (Sigma-Aldrich, St. Louis, MO). Images were taken with an iPhone 6 camera under auto-exposure settings using a white background, and densitometry was performed with ImageJ.

M13 Phage-Antibody Conjugation

1 μL of 2.8 mg/mL polyclonal anti-hCG antibody (1.1×10^{13}) was modified with 1 μL of 0.1 mg/mL Traut's Reagent (Thermo Fisher Scientific, #26101) in de-ionized (DI) water and 128 μL of 5 mM EDTA/PBS (pH 8.0). The mixture was

incubated for 1 hour on a rotator at room temperature and then applied to a 7 KDa (MWCO) Zeba spin desalting column (Thermo Fisher Scientific, #89882). Concurrently, 100 µL of ~10^{12} phage /mL in PBS was modified with 10 µL of 1 mg/mL succinimidyl 4-(N-maleimidomethyl) cyclohexane-1-carboxylate (SMCC) and 20 µL of PBS (pH 7.0). The mixture was incubated for 30 minutes on a rotator at room temperature and then applied to a 7 KDa Zeba column. After both mixtures passed through the Zeba columns, they were combined and incubated for 2 h on a rotator at room temperature. PBS was added to bring the total volume to 1 mL. The solution was dialyzed against 1 L of PBS with a Float-A-Lyzer 300 KDa MWCO dialysis cartridge (Fisher Scientific, #08-607-029) with five complete buffer changes over 36 hours.

Blood Filter Evaluation

The sample pads of LFA strips assembled as previously described, were replaced with blood filters from the following manufacturers: mdi membrane technologies, (FR1 (0.35 mm), FR1 (0.6 mm), FR2 (0.7 mm), and WFR1), GE Healthcare (Fusion 5 and MF1), Vivid Plasma (GX and GR), and PrimeCare (SG, NX, and X). 50 µL of whole blood (Gulf Coast Regional Blood Center with EDTA anticoagulant) was added at the beginning of each filter. After two minutes, strips were washed three times with 20 µL washing buffer (1% PBS, 0.5 % TWEEN-20, 0.5% BSA). Images were taken with an iPhone 6 camera under auto-exposure using a white background, and densitometry was performed with ImageJ to determine the amount of blood that passed the conjugate release pad.

Detection of hCG in Blood

Various dilutions of hCG in 50 μL of whole blood (Gulf Coast Regional Blood Center) and was added at the beginning of the blood filter. After two minutes, strips were washed three times with 20 μL of washing buffer (1% PBS, 0.5 % TWEEN-20, 0.5% BSA). 20 μL of anti-M13 HRP diluted in 1% PBS, 0.5 % TWEEN-20, 0.5% BSA was added. Strips were then washed five times with 20 μL of washing buffer. Signals were visualized by spotting 5 μL TMB liquid substrate onto the membrane spot (Sigma-Aldrich, St. Louis, MO). Images were taken with an iPhone 6 camera using auto-exposure using a white background, and densitometry was performed with ImageJ[119].

Storage and Stability Tests

LFA strips were assembled as previously described with the selected blood filter, conjugate release pad, membrane, and absorbent pad. Strips were stored in LFA cassettes (mdi Membrane) and were packaged in mylar bags (QQ-Studio) with silica gel desiccant (Interteck Packaging), and vacuum sealed (Sinbo DZ-280/2SE). Sealed bags were stored at 37°C and tested for the detection of hCG in blood as previously described every seven days over the course of 28 days.

Results and Discussion

The increased sensitivity previously demonstrated with M13 phage as reporter particles make evaluation of long-term storage stability, integration into complete tests, and use in clinically-relevant samples of great interest. Reporter particles incorporated into the strip is a key way to reduce the number of steps and minimize

test error. A truly POC platform is one that requires minimum user intervention, so only sample addition is need[120]. Reporter particles implemented into an LFA need to undergo further optimization to ensure sensitivity is maintained as various factors may affect the assays' sensitivty[121]. For practical use, LFA strips must be packaged and perform consistently over the course of an extended shelf-life. To determine the incorporation of M13 phage into LFA strips, a buffer for stable storage and release of the phage was investigated. Additional criteria considered in LFA strip development such as the membrane type, the buffers, and antibody immobilization on the membrane. We describe the development of a rapid and sensitive lateral flow assay, and demonstrate its stability and use in blood through the optimization of lateral flow components.

Evaluating Viral-Nanoparticle Lateral Flow Assays (LFAs)

To evaluate phage as reporter particles, complete LFA strips were fully assembled, including sample pad, conjugate release pad, membrane, and absorbent pad. Previous experiments that demonstrated phage as a reporter particle used strips that didn't implement a conjugate release pad. Improper overlap of the conjugate release pad by the sample pad or by the membrane is known to affect the flow and subsequently can affect the assays' sensitivity[122]. Regions of overlap between each part of the membrane were chosen at 2 mm and were consistent for each overlap. To ensure detection of phage was not affected by membrane overlap, strips with the conjugate release pad were evaluated with flow beginning at the top of the sample pad (Fig. 16B). For screening experiments, no control line was added to the strip. A signal

was obtained by the binding of phage on an anti-M13 capture line, followed by binding of anti-M13-HRP and addition of chromogenic, TMB resulting in a colorimetric readout (Fig 16A). No significant differences in detection of M13 phage were observed with the incorporation of the conjugate release pad.

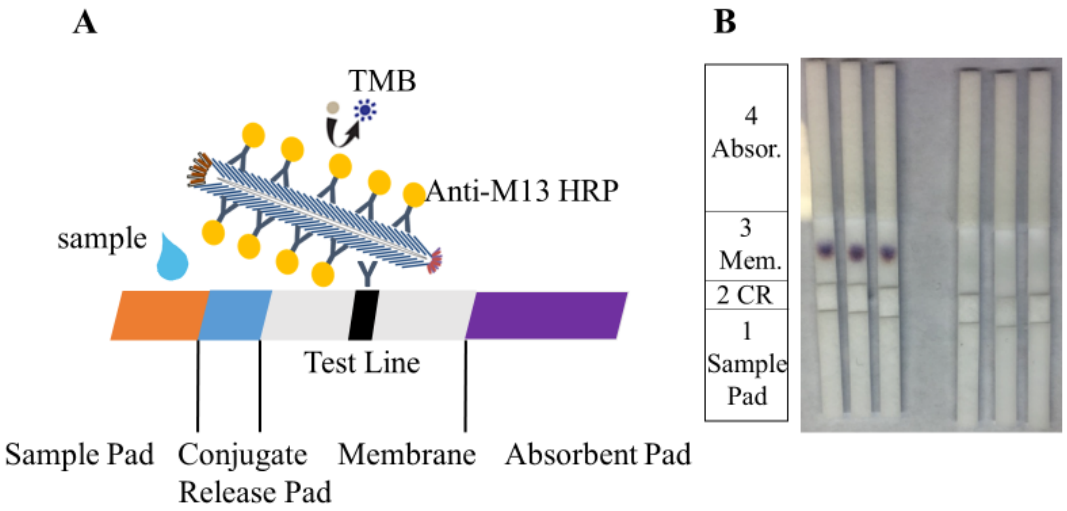

Figure 16: *Lateral Flow Assay with Viral Nanoparticles. A) Bacteriophage lateral flow assay schematic. B) LFAs ran with bacteriophage with a conjugate release pad.*

Schematic of a bacteriophage lateral flow assay, with test and control lines. No conjugate release pad is shown in the schematic (Fig 16A). LFA of bacteriophage with conjugate release pads (Fig. 16B). 0.5 µL of 4.3 mg/mL anti-M13 antibody in 50 mM sodium acetate, pH 3.6, was spotted on the membrane and allowed to air-dry for 24 h. Strips were washed two times with 20 µL of washing buffer (1% PBS, 0.5 % TWEEN-20, 0.5% BSA). 20 µL of M13 (10^{10} phage/mL) was passed through the strip, and then washed 3 times with 20 µL of washing buffer. 20 µL of anti-M13 HRP with a 1:4,000 dilution in 1% PBS, 0.5 % TWEEN-20, 0.5% BSA was added. Strips

were then washed five times 20 µL each and allowed to dry for 5 minutes. Signals were visualized by spotting 5 µL TMB liquid substrate onto the test spot. Stripes were imaged with an iPhone 6 camera under auto-exposure settings. A strip without M13 phage served as the negative control. 1 indicates the sample pad, CR indicates the conjugate release pad, Mem is the membrane, and Abs being the absorbent pad. Only a test line was spotted.

Lyophilization of Phage LFAs

For incorporation of bacteriophage into the conjugate release pad, various excipients were examined, to have a minimal step assay. Excipients are added to the conjugate release pad to stabilize and promote the re-solubilization of the reporter conjugate and minimize adsorption of the analyte to the membrane. The addition of reporter particles into conjugate release pads is followed by a drying or lyophilization process, which is crucial for the storage and release of reporter conjugated particles.[40]. To overcome variability during reporter particle integration, lyophilization, also known as freeze-drying, is commonly applied and is known to increase the speed and sensitivity of lateral flow assays[123]. The type of excipient used can affect the protein structure and function, so the excipient formulation needs to be optimized for each protein[124]. The buffers and sugars chosen for the storage of bacteriophage on conjugate release pads were based on previous dried-protein storage studies[125]. Succinate and citrate were chosen at a concentration of 50 mM along with 5% lactose or trehalose. These excipients were compared with water and PBS in both air-dried and lyophilized strips and served as a starting point to determine if more excipients would need to be

screened (Fig 17). Complete lateral flow strips were used for optimization, and excipient characterization was based on the release of M13 and anti-M13 HRP reacting with TMP resulting in a colorimetric readout at the capture line. As a control a set of strips was run with excipients and no phage.

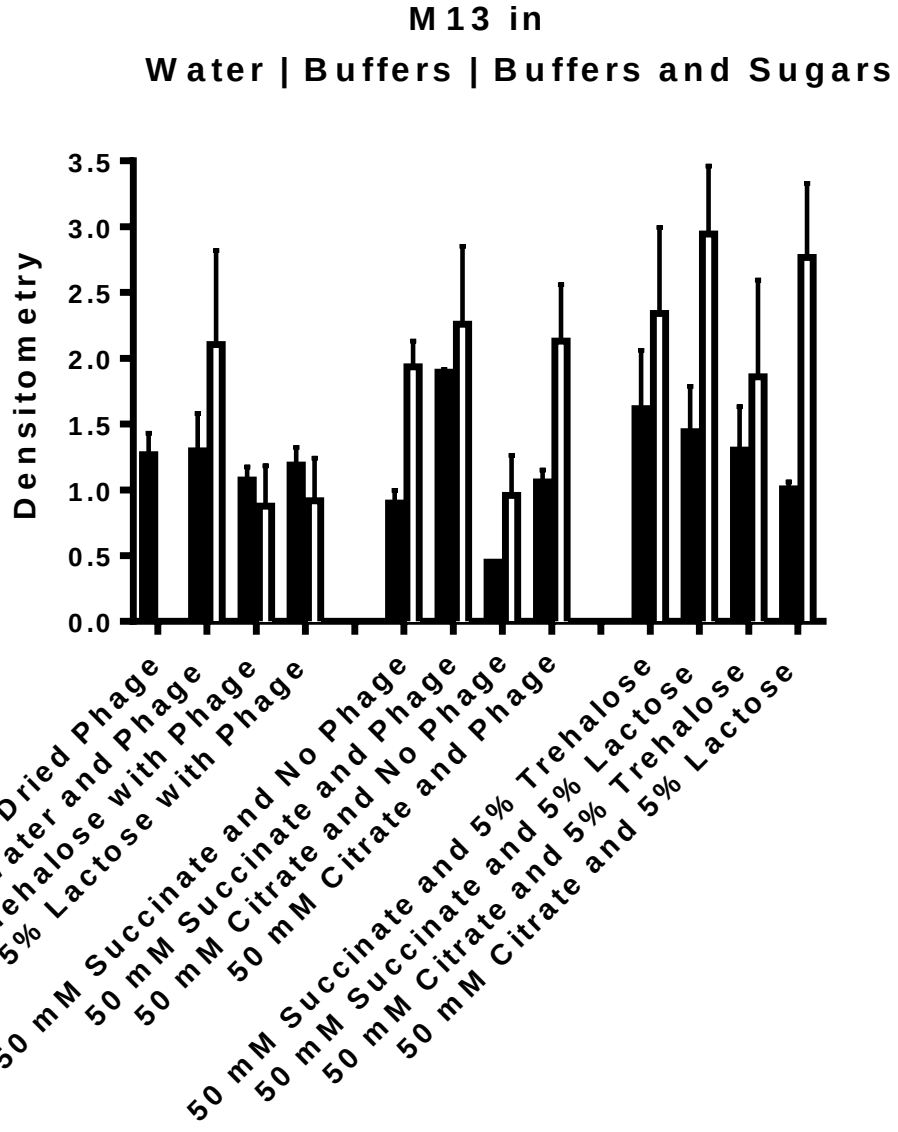

Figure 17: *Conjugate Release Pad Buffer Optimization*

Figure 17 demonstrates strips that were dried in two different conditions (black bars represent air-dried, and white bars represent freeze-dried). 3 µL of bacteriophage (10^7 pfu/ml) diluted in various buffers was spotted on the conjugate release pad (Fusion 5) and then were freeze or air-dried. Strips were washed four times with 20 µL of 1% PBS, 0.5 % TWEEN-20, 0.5% BSA. 20 µL of anti-M13-HRP 1:4,000 dilution in wash buffer was added, followed by 5 washes of 20 1% PBS, 0.5 % TWEEN-20, 0.5% BSA. The strips were allowed to air-dry for 5 minutes, followed by the application of TMB. Images were taken by an iPhone 6 camera using an auto-exposure setting, and densitometry was performed using ImageJ. For buffers, succinate or citrate was dissolved in water at a concentration of 50 mM with 5% lactose or trehalose. For each condition, a set of 3 strips were stored with an excipient and run without phage as a negative control. M13 was added to the conjugate release pad (Fusion 5) in water or a 50 mM citrate buffer, or a 50 mM succinate buffer. Other conditions were 50 mM succinate buffer with 5% trehalose, or 5% lactose. The other buffer was a 50 mM citrate buffer with 5% trehalose or 5% lactose (n=3; ± SEM).

Throughout the optimization experiments, freeze-drying the bacteriophage produced a greater colorimetric readout. (Fig 17). There were no observable impacts on the effects of HRP or TMB for the colorimetric readout in the presence of excipients. Overall in terms of buffer selection, the ones that yielded the strongest signal were 50 mM citrate with 5% lactose and 50 mM succinate with 5% lactose (Fig 17). For further optimization, M13 storage with 50 mM citrate and 5% lactose was

chosen due to the colorimetric signal being sharper, not diffuse, and spotty compared to 50 mM succinate with 5% lactose.

Conjugate Release Pad Optimization

The complete release of the reporter particle from the conjugate release pad is crucial for a sensitive test, so further optimization is required beyond buffer screening. Conjugate release pads need to be optimized to determine which pad ensures proper liquid flow and analyte detection. In the buffer optimization experiments, Fusion 5 was used as the conjugate release pad, as it can be implemented for every part of the strip[126]. Fusion 5 was compared to nitrocellulose (FF80HP Plus) and Standard 14, a thinner glass fiber compared to Fusion 5. 3 µL of M13 (10^7 pfu/mL) was added to the conjugate release pad in a 50 mM citrate 5% lactose buffer or in PBS, and strips were freeze and air-dried. Control strips had excipient and no phage to ensure there was no cross-reactivity and non-specific binding from the excipients. Strips were run with four washes of 20 µL of 1% PBS, 0.5 % TWEEN-20, 0.5% BSA, followed by 20 µL of anti-M13 HRP conjugate, and 5 washes of 20 µL 1% PBS, 0.5 % TWEEN-20, 0.5% BSA. Strips were allowed to dry for 5 minutes before TMB was spotted at the conjugate release pad and the test line. Conjugate release pads were compared by the intensity of the colorimetric readout at the membrane and at the conjugate release pad. Freeze-dried bacteriophage still yielded the strongest signal when compared to air drying (Fig 18A and 18B). Through testing various conjugate release pads, Standard 14 demonstrated the strongest colorimetric readout at the test line with a minimal readout at the conjugate release pad (Fig. 18C). After optimizing the conjugate release

pad and excipient formulation, the rest of the membrane components were further examined. The sample pad and membrane consisted of Fusion 5 in which we demonstrated a consistent flow of bacteriophage. Nitrocellulose was considered as the membrane; however, we have observed a sharper colorimetric readout on Fusion 5. As for the absorbent pad, Fusion 5 and CF5, a cotton linter material, were compared, and the latter could hold more volume, which is suitable for extra washes.

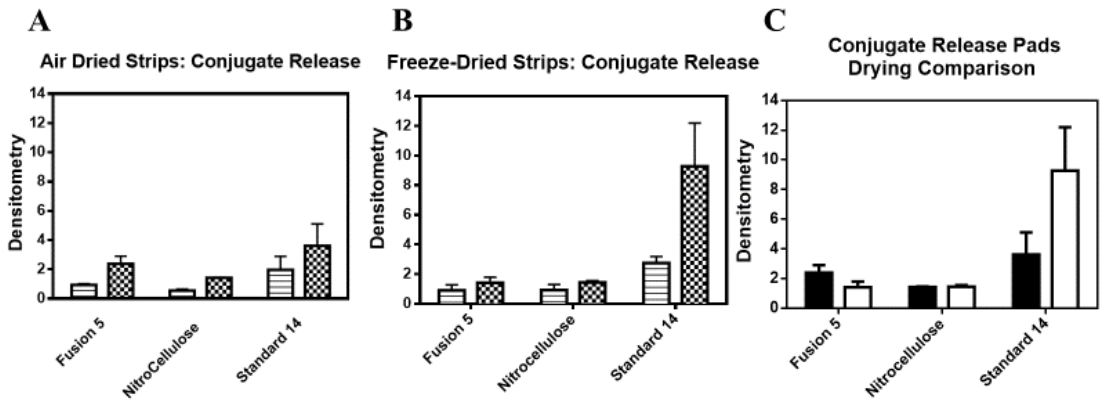

Figure 18: *Conjugate Release Pad Optimization. A) Strips dried on lab bench at ambient temperature. B) Strips that were freeze-dried. C) Comparison of strips that were air and freeze-dried.*

Figures 18A-C demonstrate strips that were dried in two different conditions (lined bars represent M13 in PBS, checkered bars represent M13 in 50 mM citrate and 5% lactose, black bars represent air-dried strips, and white bars represents freeze-dried strips) and were run with bacteriophage (10^7 pfu/ml). First, four washes of 20 µL 1% PBS, 0.5 % TWEEN-20, 0.5% BSA followed by 20 µL anti-M13-HRP diluted in washing buffer were performed. This was followed by five 20 µL washes of 1% PBS, 0.5 % TWEEN-20, 0.5% BSA, and a drying time of 5 minutes. A chromogenic

substrate (TMB) was spotted on the membrane to result in a colorimetric readout. Images were taken by an iPhone 6 camera under auto-exposure, and densitometry was performed using ImageJ. For buffers, PBS and 50 mM citrate with 5% lactose were compared. For each condition, a set of 3 strips were stored with an excipient and run without phage. Air-Dried Strips. M13 was added to the conjugate release pad, Fusion 5, Nitrocellulose, and Standard 14 in PBS or 50 mM citrate 5% lactose buffer, and strips were dried on the lab bench (Fig. 18A). Freeze-Dried Strips. M13 was added to the conjugate release pad, Fusion 5, Nitrocellulose, and Standard 14 in PBS or 50 mM citrate 5% lactose buffer, and strips were freeze-dried (Fig. 18B). Comparison of conjugate release pads that were air and freeze-dried (Fig. 18C). Comparison of M13 added to varying conjugate release pads in 50 mM citrate 5% lactose buffer in which strips were air or freeze-dried. A set of 3 strips were run for each condition and graphed with the standard error.

Cassette Integration

Buffer and strip optimization were performed with non-conjugated viral nanoparticles. For analyte detection, M13 phage were functionalized with anti-hCG antibodies, as hCG assays have been extensively studied. The functionalized viral nanoparticles were spotted on the conjugate release pad with the selected excipient formulation, and strips were air or freeze-dried (Fig. 19). The strongest signal readout is demonstrated using a citrate and lactose buffer, and with, freeze-dried strips (Fig. 17). For each buffer condition, a set of strips were freeze-dried with excipient and

phage anti-hCG conjugate but run without hCG to ensure no cross-reactivity and non-specific binding from the M13 phage-conjugate.

Towards practical use, LFA strips were packaged into cassettes to ensure strip integrity and to minimize sample handling[127,128]. This was demonstrated using an M13 anti-hCG conjugate, which was stored in the conjugate release pad. The signal forms by hCG being added to the beginning of the strip, which binds to the M13 anti-hCG conjugate and migrates along the strip and binds to anti-hCG antibodies immobilized on the membrane. At this spot, it is a sandwich stack. Anti-M13 HRP is added and migrates through the strip followed by the application of TMB. As a control, strips were run without hCG, and thus, any M13 anti-hCG conjugate should pass by the immobilized anti-hCG antibodies (Fig. 19B). The signal is from the non-specific binding of anti-M13 HRP to the membrane; thus, if a lower control value is needed, the number of washing steps needs to be increased, an increase in the surfactant buffer, or pre-treatment of the LFA strip. While we demonstrated the use of functionalized viral nanoparticles on an LFA strip, we assembled them into plastic cassettes and further tested them (Fig. 19C). From these freeze-dried buffer optimization experiments, we were able to validate the use of functionalized viral nanoparticles in LFAs.

Figure 19 A-C demonstrate strips that were dried in two different conditions (black bars represent air-dried and white bars represents freeze-dried) with bacteriophage (10^7 pfu/ml) chemically modified to anti-hCG antibodies and stored in

the conjugate release pad. M13 anti-hCG conjugate was stored in water, PBS, or with 50 mM citrate and 5% lactose.

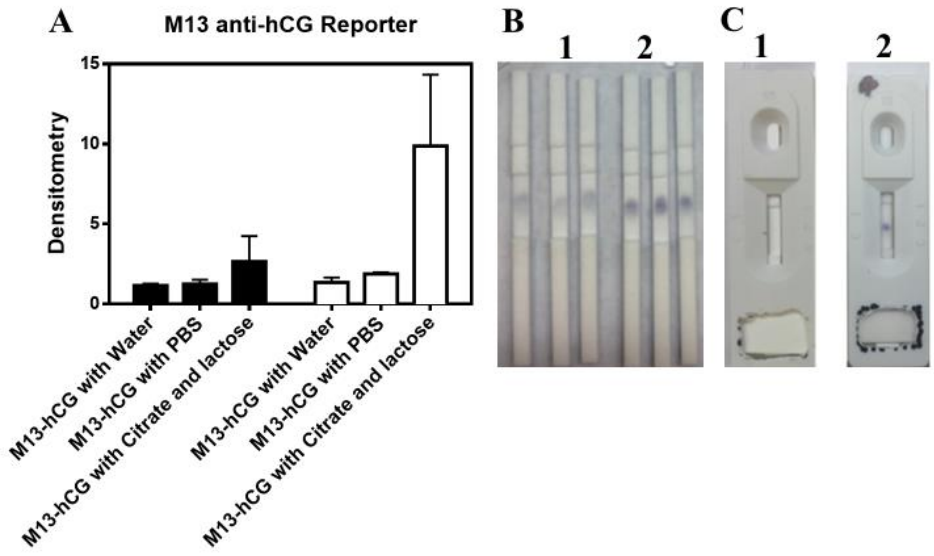

Figure 19: *M13 anti-hCG Reporter LFA Optimization. A) Densitometry of strips that were air and freeze dried with varying excipients. B) Strips ran and without M13 anti-hCG conjugate. C). Strips incorporated into plastic cassettes*

20 µL of 5 ng/mL of hCG in wash buffer (1% PBS, 0.5 % TWEEN-20, 0.5% BSA) was added at the sample pad followed three sets of 20 µL wash buffer. Next, 20 µL of anti-M13-HRP diluted in 1% PBS, 0.5 % TWEEN-20, 0.5% BSA was passed through the strip, followed by 5 washes of 20 µL 1% PBS, 0.5 % TWEEN-20, 0.5% BSA and a drying time of 5 minutes. A chromogenic substrate (TMB) was spotted on the membrane to result in a colorimetric readout. Images were taken by an iPhone 6 camera under auto-exposure, and densitometry was performed using ImageJ. For each condition, a set of 3 strips were stored with an excipient and run without phage. M13 anti-hCG conjugate was added to the conjugate release pads (Standard 14) in a 50 mM citrate 5% lactose buffer, water or PBS (Fig. 19A). Readout of conjugated viral

nanoparticles. Strips ran with M13 anti-hCG conjugate and without hCG (1) and with hCG (2) (Fig. 19B). Integration of conjugated viral nanoparticles into cassettes. LFA strips were packed into cassettes with M13 anti-hCG conjugate stored in the conjugate release pad and ran without (1) and with (2) hCG (Fig. 19C).

Blood Filter Optimization

Filtering of whole blood is critical for analyte detection in assays, and multiple approaches have been demonstrated from self-powered systems to external devices, and paper membranes[129–131]. Many analytes are present in blood from viruses, Ig molecules, and small molecules, among others. For colorimetric LFAs, blood obscures the signals, and blood filters have been used due to being asymmetric for the capture red blood cells and allow plasma to flow through. Blood filters have a limited capacity and can cause cells to lyse, so we tested a variety of blood filters from different suppliers currently on the market to determine the filter with the highest blood capacity for an M13 phage LFA.

While the blood filters reported a capacity of 40-50 µL of whole blood, upon further testing, the capacity didn't hold up due to red blood cells breaking through the filter and eventually flowing through the rest of strip (Fig. 20A and 20B). Fusion 5 membrane that is marketed for implementation of all of the strip caused the red blood cells to lyse, resulting in the strip turning a dark red color. From a total of 10 blood filters, only four were further tested to determine which had the highest capacity under assay conditions due to their ability to hold 50 µL of blood within the filter (Fig. 20C). The six blood filters were further tested with washing after the addition of blood and

caused red blood cells to escape from the filter and lyse and obscure the colorimetric signal Studies were performed by running an LFA with M13 in blood for four filters. Again, with washing, colorimetric detection is possible, but the red blood cells escaped from the filter and were lysed obscuring detection. Visualization of a colored spot on the membrane is difficult on colored backgrounds compared to a white background. Based on these tests, FR2 (0.7 mm) had the clearest membrane background for easier colorimetric detection by the naked eye (Fig. 20C).

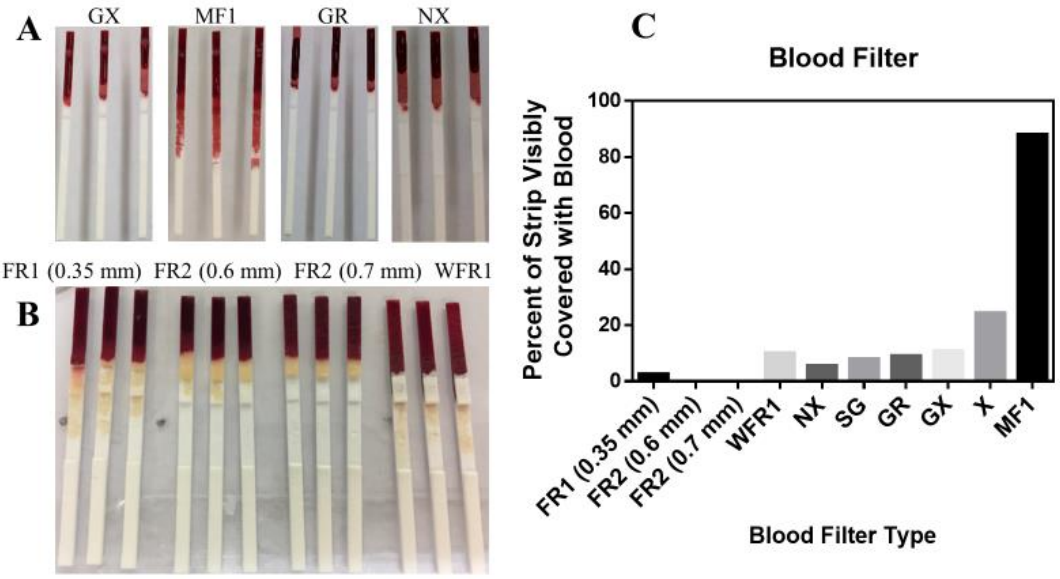

Figure 20: *Blood Filter Performance. A and B) Blood filter retention from various manufactures. C). Percent of blood that covered the strip from the filter.*

50 µL of whole blood was added to the beginning of each strip. Blood filter capacity from different manufacturers, from left to right (GX, MF1, GR, and NX) (Fig. 20A). Blood filters from mdi Membrane, from left to right (FR1 (0.35 mm), FR2 (0.6 mm), FR2 (0.7 mm), and WFR1 (Fig. 20 B).

Strips were fitted with the selected blood filter (FR2 (0.7 mm)) and freeze-dried with 50 mM citrate and 5 % lactose and with M13-anti-hCG conjugate stored in the conjugate release pad. This allowed for the demonstration of a fully integrated LFA for the detection of hCG and its performance in blood (Fig. 21A).

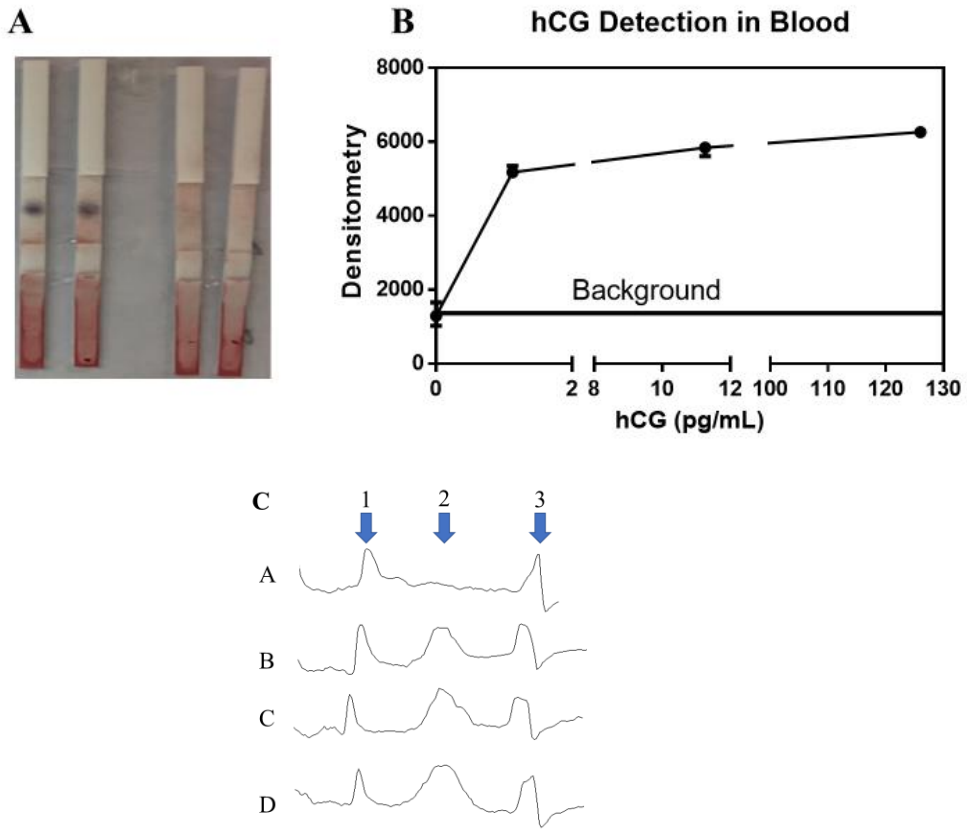

Figure 21: *M13 anti-hCG Conjugate Performance in Blood. A) M13 anti-hCG conjugate strips ran in blood with hCG. B) Densitometry of strips based on the detection of hCG in blood. C) Plot profiles from densitometry.*

A variety of hCG dilutions spiked in blood were used to determine the LFA's sensitivity using conjugated viral nanoparticles. Through image analysis and densitometry, the limit of detection was 1 pg/mL in blood (Fig 21B and 21C). The signal is 30% higher than 3 times the standard deviation of the background signal, a standard for the limit of detection. Thus, a lower limit is potentially possible. The low

level of detection is possible by matrix effects of the bacteriophage interacting with the blood and its particulates, but this needs further analysis. Long polymers are known to increase the flux of red blood cells in capillary walls[132]. While the red blood cells are caught in the blood filter, the aspect ratio of phage may allow it to interact with particulates in blood and the analyte contributing to the detection level. Additionally, plasma and serum are known to reduce non-specific binding. From these studies, we were also able to determine the blood filter performance was not impacted by the strip undergoing the freeze-drying process.

Strips were freeze-dried with the incorporation of M13-anti-hCG conjugate (3 µL of 10^7 pfu/ml) (Fig. 21A). 112 pg/mL of hCG was spiked into 50 µL of blood and added to the sampled pad. After two minutes, there were three 20 µL washes of 1% PBS, 0.5 % TWEEN-20, 0.5% BSA, and the addition of 20 µL anti-M13-HRP diluted in wash buffer, followed by five 20 µL washes of 1% PBS, 0.5 % TWEEN-20, 0.5% BSA. The strip was allowed to dry for 5 minutes, and TMB was added. Images were taken by an iPhone 6 camera under auto-exposure setting and densitometry was performed using ImageJ based on the peaks at the membrane test spot. Detection of various hCG concentrations with densitometry of the colorimetric readout with varying dilutions for the detection of hCG in blood. A set of 3 strips was run for each hCG concentration and is graphed with the standard error (Fig. 21B). Plot profiles from ImageJ densitometry: A is 0 ng/mL, B is 1 pg/mL, C is 11.2 pg/mL and D is 112 pg/mL (Fig. 21C). 1 indicates the overlap of the conjugate release pad with the

membrane, 2 indicate the test spot on the membrane, and 3 indicates the overlap of the absorbent pad with the membrane.

Storage and Stability Studies

By optimization of a freeze-dried formulation for the release of M13 anti-hCG conjugate in blood samples, a very low limit of detection was achieved. Another important attribute of a useful assay is the storage stability of LFA strips[123]. To characterize the shelf-life of LFA strips with conjugated viral nanoparticles and blood filters, an accelerated stability study was performed. Assembled strips were packaged into cassettes and stored with desiccant (Interteck Packaging), which was sealed into mylar pouches (QQ Studio). LFAs have suffered limited sensitivity from the influences of environmental conditions (temperature and relative humidity)[133]. LFA strips were stored in a 37℃ incubator to test the stability of the detection of hCG in blood. During LFA strip storage, a partial unfolding of the immobilized antibody or the antibody being cleaved off from the phage is possible[134–136]. Additionally, there could be damage to phage in the process. Every 7 days, strips packaged in cassettes and pouches were removed for the detection of hCG in blood (Fig. 22). Two concentrations of hCG were chosen, 1 ng/mL, (an hCG concentration detected by gold LFA tests), and, 134 pg/mL, lower but above the limit of detection reported by our LFA test[137–140]. The detection of 134 pg/mL hCG was stable over 28 days, while the 1.34 ng/mL hCG detection was more variable. The higher variability can be due to a higher analyte concentration and interference with the membrane and sample. Additionally, at higher concentrations of hCG, a stronger signal is observed at the

membrane, which was observed across the two concentrations. Across the 28 days, strips did not fail, and the detection of hCG in blood was stable over time. The storage of LFA strips with conjugated viral nanoparticles and blood filters demonstrated stability for the detection of hCG over the course of 28 days.

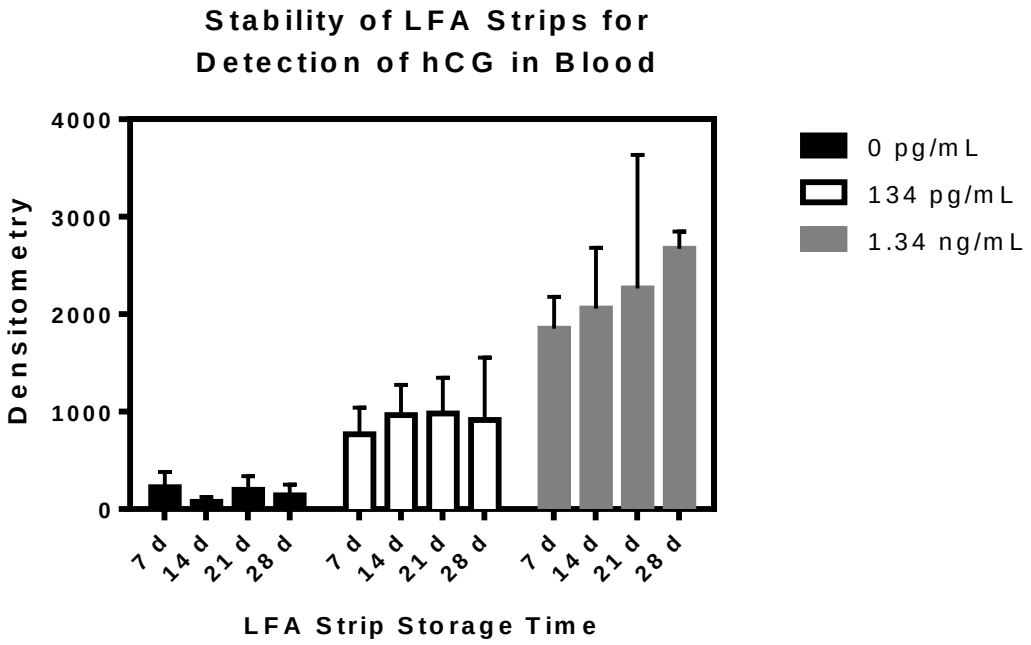

Figure 22: *Stability of LFA Strips*

LFA strips with the blood filter FR2 (0.7mm) were prepared with M13 anti-hCG conjugate in 50 mM citrate 5% lactose buffer stored in the conjugate release pad. 0.5 μL of rabbit polyclonal anti-M13 IgG antibody (4.3 mg/mL) (Novus Biologicals, Littleton, CO) was diluted in 50 mM sodium acetate buffer (pH 3.6) and spotted on the membrane. LFA strips were freeze-dried in cassettes and then packaged in mylar bags with desiccant. Assembled tests were stored in a 37℃ incubator, and were taken out every 7 days (d) for the detection of hCG in blood. Various concentrations of hCG

were spiked in 50 µL of blood. This was followed by three 20 µL washes of 1% PBS 0.5% TWEEN-20-0.5% BSA, and the addition of 20 µL anti-M13-HRP diluted in wash buffer, followed by five 20 µL washes of PBS 0.1% TWEEN-20-0.5% BSA followed by the addition of TMB. A set of 3 strips was run at each time point. Images were taken by an iPhone 6 camera using auto-exposure setting and densitometry was performed using ImageJ based on peaks at the membrane test spot.

Conclusions

Increased sensitivity among LFAs may find countless applications in medical diagnostics, food safety, forensic science, and therapeutic monitoring, etc. The integration of M13 phage as a reporter particle into complete LFA tests was investigated, and a freeze-drying formulation for the optimal release from conjugate release pads was identified. These studies did demonstrate that freeze-drying strips were better than air-dried strips. Additionally, various conjugate release pads were tested for an M13 phage conjugate LFA. From these results, we were able to demonstrate LFA strip integration in cassettes. The incorporation of M13-conjugated phage into LFAs and cassettes further allowed us to develop a complete assay for the detection of human chorionic gonadotropin (hCG) and demonstrated our assays' performance in blood. By testing various blood filters to determine the highest blood capacity under assay conditions, we achieved a limit of detection of 1 pg/mL in blood. Storage and worldwide shipping at ambient temperature are concerns for POC applications in remote and resource-limited environments[69]. Additionally, a brief accelerated stability study indicated that using conjugated viral nanoparticles and the

LFA strip is stable over a month for the detection of hCG in blood. To determine the full shelf-life of LFA tests, long term studies need to be performed. Thus, for a rapid and sensitive lateral flow assay, whether, in buffer or blood, M13 bacteriophage as a reporter has significant advantages and can lead to an increased sensitivity among LFAs. To further minimize user intervention, a colorimetric readout can be replaced with a lyophilized chemiluminescent substrate or enzyme-based reagent systems to further minimize steps[141,142].

We were able to further validate M13 phage incorporation for a complete assay and demonstrated a detection limit of 1 pg/mL. In turn, this suggests that careful tuning of membrane design variables such as proper membrane selection and storage buffer can increase binding efficiency and thus the sensitivity of LFAs[143–146]. In the future, we will examine the shelf life of other conjugation possibilities for LFAs, and their use in other sample mediums needs to be tested, such as saliva, urine, and stool. More broadly, our development and testing of an M13 phage LFA may prove useful towards the detection of biomarkers and analytes, where an increased sensitivity is needed in LFAs.

CHAPTER 4: CONCLUSIONS AND FUTURE DIRECTIONS

Conclusions and Future Directions from the Lyophilization M13 Phage

LFAs are diagnostic tools, and increasing their sensitivity will allow them to be useful in a variety of fields where rapid detection is a priority. They are affordable tests that are convenient, do not require the use of trained personnel, and can be used in resource-limited regions. For the detection of low-level analytes, proteins, small molecules, and chemicals, among others, LFAs need to demonstrate high sensitivity and low limits of detection. For improving the sensitivity of the assay, researchers have focused on antibody selection, the type of reporter particle, adding an external device, and the assays' format, whether an LFA, dipstick, or wax paper microfluidic strip. For each case, there are certain advantages and disadvantages in improving the sensitivity of an assay. However, improving the sensitivity may result in an increased cost of the assay or the need for trained personnel or laboratory equipment that are not commonly found in certain regions. There can be a trade-off between the sensitivity and the practicality of the assay where it is being deployed.

The selection of the reporter particle plays a critical role in LFAs, both in how the assay is run and its readout. From previous studies, M13 phage was demonstrated as an LFA reporter particle with increased sensitivity compared to gold nanoparticles in the detection of hCG and detection of norovirus[49,50]. We investigated whether M13 phage could be implemented into a complete LFA and be stable over an extended shelf life. We further validated M13 phage as a reporter particle and demonstrated a freeze-drying excipient formulation for the storage and release of M13 phage.

Additionally, we developed a complete LFA assay for the detection of hCG in buffer and in whole blood.

We were able to determine the parameters that needed to be tuned to ensure a rapid, sensitive assay. The type of conjugate release pad affects the flow of M13 phage and readout of the assay[44]. Furthermore, strip components were optimized, including the sample pad, conjugate release pad, membrane, and absorbent pad. Freeze-drying LFA strips allowed for the detection of hCG using conjugated M13 phage without signal interference from the excipient formulation. Minimal non-specific binding was exhibited after freeze-drying of strips and conjugated M13 phage. The incorporation of conjugated M13 phage reduced a key operator step in running the LFA. An assay with minimal steps will have reduced error and can facilitate trained personnel performing the assay[42]. Additionally, to protect the sample medium and assay from contamination, lateral flow strips were incorporated into plastic cassettes and shown to perform consistently. To demonstrate the use of LFAs with clinically-relevant samples, a series of commercial blood filters were evaluated, and one was selected that demonstrated the highest blood capacity. Expanding on optimization of LFA strips, we demonstrated a whole-blood limit of detection for hCG of 1 pg/mL. To address the stability of phage LFAs, a brief one-month storage stability study was performed with the selected lateral flow strip components assembled into plastic cassettes and vacuum-sealed along with desiccant packages in mylar pouches. Tests were stored at 37°C for one month, then tested for the detection of two concentrations of hCG in blood, and performed consistently. Minimal assay variability was observed at lower

hCG concentrations, while more variability was observed at the higher concentration, possibly due to analyte interference. For a rapid and sensitive lateral flow assay, whether, in buffer or blood, M13 bacteriophage as a reporter has demonstrated advantages and can lead to an increased sensitivity among LFAs.

There is a need for increased sensitivity of LFAs for the detection of analytes or molecules. There are countless applications from medical diagnostics, food safety, forensic science, therapeutic drug monitoring, etc. Through the characterization of viral nanoparticles, we were able to further validate them as reporter particles and their use in a complete assay across two different mediums and demonstrated a detection limit of 1 pg/mL. While more characterization is required, we believe that using viral nanoparticles can lead to increased sensitivity among LFAs.

While we demonstrated the optimization of a freeze-dried formulation and an optimal blood filter, the storage and stability of LFA strips with conjugated viral nanoparticles need to be characterized for longer time periods. Packaged strips would be stored at 37℃ and at ambient temperature for 18 months, with regular interval testing to ensure the detection limit is maintained across the desired shelf life. Various factors can affect the stability of the reporter particle, the conjugated recognition elements, the immobilized antibodies, and the LFA membrane[134,135,147]. While whole blood was tested in LFAs with conjugated M13 phage, other sample media need to be tested, such as saliva, urine, and stool, to determine any systematic matrix interferences. Additionally, blood with various anti-coagulants needs to be tested, as these can affect signal readout[148]. While a low limit of detection was obtained with

M13 phage conjugated to anti-hCG antibodies, other chemical modalities and analyte detection need characterization. Due to the high aspect ratio of M13 phage, it tumbles in lateral flow and gets caught in the pores of the matrix, requiring further strip washing. Currently, there are multiple wash steps involved, extending assay time, and creating chances for error. Ideally, washing with a few drops from a pipette commonly seen in pregnancy test is a future aim[149]. Testing different chase buffers for minimal washing is an aim to have an assay meet the "user-friendly" of ASSURED criteria set by WHO.

Throughout these experiments, M13 phage was conjugated to antibodies for the detection of analytes through a colorimetric readout. The possibility of a chemiluminescent or fluorescent readout with M13 phage needs investigation in order to determine the applicability of such readouts and their detection limits. The introduction of smartphones and handheld devices for LFA measurements with M13 phage can lead to a lower detection limit and a greater degree of sensitivity that needs further examination. M13 phage can also be conjugated to other enzymes or use alternative reporters and substrates. The incorporation of M13 phage into LFAs does not add an increased cost to the assay that would affect its deployment in resource-limited regions. M13 phage can be bought in bulk or reproduced in *E.coli*. Compared to an LFA test that employs gold nanoparticles, M13 phage is a practical affordable reporter.

We demonstrated M13 phage could provide low detection limits in LFAs, but the mechanisms of capture and binding are not fully understood. One way to

understand the binding mechanism is through techniques such as surface plasmon resonance (SPR), biolayer interferometry (BLI), and stopped-flow fluorescence. Rapid filtration allows for the measurement of capture in porous matrices that will facilitate parameter tuning in LFAs. Understanding the capture mechanisms of M13 phage in porous matrices will allow sensitivity enhancements and detection limits of LFAs. Additionally, rapid filtration will allow us to understand how the aspect ratio of M13 phage may assist in achieving the observed low detection limits. With M13 phage being able to be genetically modified, the use of phages with different aspect ratios will allow further understanding of phage capture in porous matrices and how it can lead to sensitive assays. Also, various researchers have conjugated multiple phages to each other for building scaffolds[150,151]. The ability to conjugate multiple phages in various shapes may further allow enhanced detection in LFAs.

While M13 phage was demonstrated in LFAs, their use in other assays needs to be considered including ELISAs, and wax-based and vertical-flow assays. Vertical-flow assays offer key advantages over their lateral-flow counterparts from reduced assay time, ability to be multiplexed, and greater sample volume. Vertical-flow assays involve capture in porous matrices, and M13 phage may meet a critical need in such an assay.

Conclusions and Future Directions for Rapid Filtration

Lateral- and vertical-flow immunoassays and a variety of biosensing technologies, as well as various preparative methods, involve the flow and capture of targets and reporters in porous matrices. Here we introduced rapid filtration as a

method for measuring the capture of analytes and reporters in porous matrices on extremely short time scales and described its use in investigating ultra-sensitive LFAs using filamentous bacteriophage as reporters.

We anticipate the measurements to help understand the remarkable sensitivity of the phage-based lateral-flow test. By varying the flow rate and timing, we can understand the capture of M13 bacteriophage at low and high antibody loading rates. The capture of M13 phage in porous matrices needs further investigation. We demonstrated capture and recovery through rapid filtration with M13 phage. Initial studies indicated that a faster flow rate might assist a higher degree of capture. This is different from other reporter particles in which a slow flow rate may provide a higher degree of capture. Thus, a study of M13 phage capture in various porous matrices is needed.

The same trend was observed with M13 phage biotinylated for capture to NeutrAvidin; higher flow rates may assist in a greater degree of capture. However, a higher loading of NeutrAvidin on the membrane was needed to capture biotinylated M13 phage. The mechanisms of capture are different in each case and may indicate a higher loading might be needed in LFAs for the capture of biotin and NeutrAvidin. Further studies of both capture mechanisms with the rapid filtration technique are required to determine the optimal flow rate for capture. This will allow results from rapid filtration to provide insights for capture in LFAs and vertical flow assays using M13 phage. Extensions of these studies would be to chemically link the target element to the membrane and investigate capture, to determine if chemical linkage to the

membrane is more advantageous or not than electrostatic adsorption. While studies were performed with M13 phage, various phages with different aspect ratios can also be investigated through the rapid filtration apparatus. This will be key in determining how the aspect ratio may assist capture and allow ways to improve the detection and sensitivity when employing phage. This will allow us to optimize lateral and vertical flow conditions for a higher degree of capture and increased sensitivity.

Future aims are to adjust the phage concentration and membrane antibody immobilization to determine how capture depends on flow rate capture across a wide range of conditions. Another aim is to wash the membrane with the surfactant buffers employed in LFAs to investigate how this affects the capture. Through these studies, we will be able to further investigate and understand the mechanisms of M13 phage capture in porous matrices. To determine which will yield the highest degree of capture, we can determine the optimal flow rate, membrane antibody immobilization level, and the surfactant buffer formulation. Furthermore, any liquid can be passed through the rapid filtration apparatus, so the sample viscosity can be adjusted to determine its role in the capture of M13 phage. Various clinically-relevant samples can also be passed through the apparatus, such as blood, serum, plasma, saliva, and urine, to observe how the sample fluid affects capture. Insights from the rapid filtration technique will allow us to develop phage assays with low limits of detection and high levels of sensitivity and specificity.

Since the kinetics of interaction and capture in matrices occurs on time scales below one second, the rapid filtration method will allow us to probe further to

understand the capture of analytes and molecules. While the experiments were performed using M13 bacteriophage, the rapid filtration apparatus is versatile, allowing the use of other reporters or analytes. Future experiments will examine varied reporter particles such as phosphors and colloidal-gold particles. These studies will characterize the capture of reporters for LFA and vertical flow. This will allow us to further understand if slower or faster flow rates or reporter particles alter the degree of capture. From delving into capture mechanisms, parameter tuning can be altered for assays based on the insights into the behavior of reporter particles in the rapid filtration apparatus.

Due to the porous matrix of the rapid filtration apparatus, multiple reporter particles up to 100 μm can be investigated. Capture experiments using this technique with various reporter particles will allow a mechanistic understanding of capture in porous matrices and how flow rate and particle shape play a role. The technique can benefit the LFA field and diagnostic space where porous membranes are used. The rapid filtration apparatus also is applicable to chromatography. In chromatographic separation, porous substrates are used. The use of immobilized proteins on porous substrates for purifying monoclonal antibodies from cell culture supernatants can be investigated by how different flow rates affect capture. The insights from capture characterization at short-time scales below one second is crucial for our understanding of antibody purification. Thus, the rapid filtration apparatus can provide insights for a variety of fields where understanding capture is a critical need.

REFERENCES

1. Ming, D., Rawson, T., Sangkaew, S., Rodriguez-Manzano, J., Georgiou, P. & Holmes, A. Connectivity of rapid-testing diagnostics and surveillance of infectious diseases. *Bull. World Health Organ.* **97**, 242–244 (2019).
2. Ferguson, B. S., Buchsbaum, S. F., Wu, T.-T., Hsieh, K., Xiao, Y., Sun, R. & Soh, H. T. Genetic Analysis of H1N1 Influenza Virus from Throat Swab Samples in a Microfluidic System for Point-of-Care Diagnostics. *J. Am. Chem. Soc.* **133**, 9129–9135 (2011).
3. Grebely, J., Lamoury, F. M. J., Hajarizadeh, B., Mowat, Y., Marshall, A. D., Bajis, S., Marks, P., Amin, J., Smith, J., Edwards, M., Gorton, C., Ezard, N., Persing, D., Kleman, M., Cunningham, P., Catlett, B., Dore, G. J. & Applegate, T. L. Evaluation of the Xpert HCV Viral Load point-of-care assay from venepuncture-collected and finger-stick capillary whole-blood samples: a cohort study. *Lancet Gastroenterol. Hepatol.* **2**, 514–520 (2017).
4. Harenberg, J., Du, S., Krämer, S., Giese, C., Schulze, A., Weiss, C. & Krämer, R. Novel Methods for Assessing Oral Direct Factor Xa and Thrombin Inhibitors: Use of Point-of-Care Testing and Urine Samples. *Semin. Thromb. Hemost.* **39**, 066–071 (2012).
5. Van den Bossche, D., Cnops, L., Verschueren, J. & Van Esbroeck, M. Comparison of four rapid diagnostic tests, ELISA, microscopy and PCR for the detection of Giardia lamblia, Cryptosporidium spp. and Entamoeba histolytica in feces. *J. Microbiol. Methods* **110**, 78–84 (2015).

6. Chin, C. D., Linder, V. & Sia, S. K. Commercialization of microfluidic point-of-care diagnostic devices. *Lab. Chip* **12**, 2118 (2012).
7. Childerhose, J. E. & MacDonald, M. E. Health consumption as work: The home pregnancy test as a domesticated health tool. *Soc. Sci. Med.* **86**, 1–8 (2013).
8. Srinivas, P. R., Kramer, B. S. & Srivastava, S. Trends in biomarker research for cancer detection. *Lancet Oncol.* **2**, 698–704 (2001).
9. Celermajer, D. S., Chow, C. K., Marijon, E., Anstey, N. M. & Woo, K. S. Cardiovascular Disease in the Developing World. *J. Am. Coll. Cardiol.* **60**, 1207–1216 (2012).
10. Etzioni, R., Urban, N., Ramsey, S., McIntosh, M., Schwartz, S., Reid, B., Radich, J., Anderson, G. & Hartwell, L. The case for early detection. *Nat. Rev. Cancer* **3**, 243–252 (2003).
11. Olsen, D. & JÃ¸rgensen, J. T. Companion Diagnostics for Targeted Cancer Drugs â€“ Clinical and Regulatory Aspects. *Front. Oncol.* **4**, (2014).
12. Nayak, S., Blumenfeld, N. R., Laksanasopin, T. & Sia, S. K. Point-of-Care Diagnostics: Recent Developments in a Connected Age. *Anal. Chem.* **89**, 102–123 (2017).
13. Gregory, K. & Lewandrowski, K. Management of a Point-of-Care Testing Program. *Clin. Lab. Med.* **29**, 433–448 (2009).
14. Vashist, S. K. Point-of-Care Diagnostics: Recent Advances and Trends. *Biosensors* **7**, (2017).

15. Point-of-Care Diagnostics Market by Testing, Platform, Mode & End User - 2022 | MarketsandMarkets. Available at: https://www.marketsandmarkets.com/Market-Reports/point-of-care-diagnostic-market-106829185.html. (Accessed: 7th March 2019)
16. Drain, P. K., Hyle, E. P., Noubary, F., Freedberg, K. A., Wilson, D., Bishai, W. R., Rodriguez, W. & Bassett, I. V. Diagnostic point-of-care tests in resource-limited settings. *Lancet Infect. Dis.* **14**, 239–249 (2014).
17. Khan, A., Vasquez, Y., Gray, J., Wians Jr, F. & Kroll, M. The Variability of Results Between Point-of-Care Testing Glucose Meters and the Central Laboratory Analyzer. *Arch. Pathol. Lab. Med.* **130**, 1527–1532 (2006).
18. Burd, E. M. Validation of Laboratory-Developed Molecular Assays for Infectious Diseases. *Clin. Microbiol. Rev.* **23**, 550–576 (2010).
19. Desenclos, J.-C., Bourdiol-Razès, M., Rolin, B., Garandeau, P., Ducos, J., Bréchot, C. & Thiers, V. Hepatitis C in a Ward for Cystic Fibrosis and Diabetic Patients Possible Transmission by Spring-Loaded Finger-Stick Devices for Self-Monitoring of Capillary Blood Glucose. *Infect. Control Hosp. Epidemiol.* **22**, 701–707 (2001).
20. Liu, A., Kilmarx, P. H., Supawitkul, S., Chaowanachan, T., Yanpaisarn, S., Chaikummao, S. & Limpakarnjanarat, K. Rapid Whole-Blood Finger-Stick Test for HIV Antibody: Performance and Acceptability Among Women in Northern Thailand: *JAIDS J. Acquir. Immune Defic. Syndr.* **33**, 194–198 (2003).

21. McGarraugh, G., Price, D., Schwartz, S. & Weinstein, R. Physiological Influences on Off-Finger Glucose Testing. *Diabetes Technol. Ther.* **3**, 367–376 (2001).

22. Mariani, A. J., Luangphinith, S., Loo, S., Scottolini, A. & Hodges, C. V. Dipstick Chemical Urinalysis: An Accurate Cost-Effective Screening Test. *J. Urol.* **132**, 64–66 (1984).

23. Lachs, M. S. Spectrum Bias in the Evaluation of Diagnostic Tests: Lessons from the Rapid Dipstick Test for Urinary Tract Infection. *Ann. Intern. Med.* **117**, 135 (1992).

24. Waugh, J. J. S., Clark, T. J., Divakaran, T. G., Khan, K. S. & Kilby, M. D. Accuracy of Urinalysis Dipstick Techniques in Predicting Significant Proteinuria in Pregnancy: *Obstet. Gynecol.* **103**, 769–777 (2004).

25. Devillé, W. L., Yzermans, J. C., van Duijn, N. P., Bezemer, P. D., van der Windt, D. A. & Bouter, L. M. The urine dipstick test useful to rule out infections. A meta-analysis of the accuracy. *BMC Urol.* **4**, (2004).

26. Lequin, R. M. Enzyme Immunoassay (EIA)/Enzyme-Linked Immunosorbent Assay (ELISA). *Clin. Chem.* **51**, 2415–2418 (2005).

27. Wilson, G. S. & Gifford, R. Biosensors for real-time in vivo measurements. *Biosens. Bioelectron.* **20**, 2388–2403 (2005).

28. Suchman, A. L. Diagnostic Decision: Diagnostic Uses of the Activated Partial Thromboplastin Time and Prothrombin Time. *Ann. Intern. Med.* **104**, 810 (1986).

29. Dascombe, B. J., Reaburn, P. R. J., Sirotic, A. C. & Coutts, A. J. The reliability of the i-STAT clinical portable analyser. *J. Sci. Med. Sport* **10**, 135–140 (2007).

30. *The immunoassay handbook: theory and applications of ligand binding, ELISA, and related techniques*. (Elsevier, 2013).

31. Bode, B. W., Irvin, B. R., Pierce, J. A., Allen, M. & Clark, A. L. Advances in Hemoglobin A1c Point of Care Technology. *J. Diabetes Sci. Technol.* **1**, 405–411 (2007).

32. Gallagher, A. J., Frick, L. H., Bushnell, P. G., Brill, R. W. & Mandelman, J. W. Blood Gas, Oxygen Saturation, pH, and Lactate Values in Elasmobranch Blood Measured with a Commercially Available Portable Clinical Analyzer and Standard Laboratory Instruments. *J. Aquat. Anim. Health* **22**, 229–234 (2010).

33. Gbinigie, O., Price, C. P., Heneghan, C., Van den Bruel, A. & Plüddemann, A. Creatinine point-of-care testing for detection and monitoring of chronic kidney disease: primary care diagnostic technology update. *Br. J. Gen. Pract.* **65**, 608–608 (2015).

34. Biagini, R. E., Sammons, D. L., Smith, J. P., MacKenzie, B. A., Striley, C. A. F., Snawder, J. E., Robertson, S. A. & Quinn, C. P. Rapid, Sensitive, and Specific Lateral-Flow Immunochromatographic Device To Measure Anti-Anthrax Protective Antigen Immunoglobulin G in Serum and Whole Blood. *Clin. Vaccine Immunol.* **13**, 541–546 (2006).

35. Magambo, K. A., Kalluvya, S. E., Kapoor, S. W., Seni, J., Chofle, A. A., Fitzgerald, D. W. & Downs, J. A. Utility of urine and serum lateral flow assays

to determine the prevalence and predictors of cryptococcal antigenemia in HIV-positive outpatients beginning antiretroviral therapy in Mwanza, Tanzania. *J. Int. AIDS Soc.* **17**, 19040 (2014).

36. Zangheri, M., Cevenini, L., Anfossi, L., Baggiani, C., Simoni, P., Di Nardo, F. & Roda, A. A simple and compact smartphone accessory for quantitative chemiluminescence-based lateral flow immunoassay for salivary cortisol detection. *Biosens. Bioelectron.* **64**, 63–68 (2015).
37. Dalirirad, S. & Steckl, A. J. Aptamer-based lateral flow assay for point of care cortisol detection in sweat. *Sens. Actuators B Chem.* **283**, 79–86 (2019).
38. Li, J. & Macdonald, J. Multiplexed lateral flow biosensors: Technological advances for radically improving point-of-care diagnoses. *Biosens. Bioelectron.* **83**, 177–192 (2016).
39. Qian, S. & Bau, H. H. Analysis of lateral flow biodetectors: competitive format. *Anal. Biochem.* **326**, 211–224 (2004).
40. Koczula, K. M. & Gallotta, A. Lateral flow assays. *Essays Biochem.* **60**, 111–120 (2016).
41. Tsai, T.-T., Huang, T.-H., Chen, C.-A., Ho, N. Y.-J., Chou, Y.-J. & Chen, C.-F. Development a stacking pad design for enhancing the sensitivity of lateral flow immunoassay. *Sci. Rep.* **8**, (2018).
42. Sajid, M., Kawde, A.-N. & Daud, M. Designs, formats and applications of lateral flow assay: A literature review. *J. Saudi Chem. Soc.* **19**, 689–705 (2015).

43. Common Formats Of Lateral Flow Tests - Creative Diagnostics. Available at: https://www.cd-diatest.com/common-formats-of-lateral-flow-tests_d27. (Accessed: 10th September 2019)

44. Posthuma-Trumpie, G. A., Korf, J. & van Amerongen, A. Lateral flow (immuno)assay: its strengths, weaknesses, opportunities and threats. A literature survey. *Anal. Bioanal. Chem.* **393**, 569–582 (2009).

45. Wang, J., Yiu, B., Obermeyer, J., Filipe, C. D. M., Brennan, J. D. & Pelton, R. Effects of Temperature and Relative Humidity on the Stability of Paper-Immobilized Antibodies. *Biomacromolecules* **13**, 559–564 (2012).

46. Dunbar, B. S. & Schwoebel, E. D. [49] Preparation of polyclonal antibodies. in *Methods in Enzymology* **182**, 663–670 (Elsevier, 1990).

47. Bradbury, A. & Plückthun, A. Reproducibility: Standardize antibodies used in research. *Nature* **518**, 27–29 (2015).

48. Armbruster, D. A. & Pry, T. Limit of blank, limit of detection and limit of quantitation. *Clin. Biochem. Rev.* **29 Suppl 1**, S49-52 (2008).

49. Adhikari, M., Dhamane, S., Hagström, A. E. V., Garvey, G., Chen, W.-H., Kourentzi, K., Strych, U. & Willson, R. C. Functionalized viral nanoparticles as ultrasensitive reporters in lateral-flow assays. *The Analyst* **138**, 5584 (2013).

50. Hagström, A. E. V., Garvey, G., Paterson, A. S., Dhamane, S., Adhikari, M., Estes, M. K., Strych, U., Kourentzi, K., Atmar, R. L. & Willson, R. C. Sensitive Detection of Norovirus Using Phage Nanoparticle Reporters in Lateral-Flow Assay. *PLOS ONE* **10**, e0126571 (2015).

51. Paterson, A. S., Raja, B., Mandadi, V., Townsend, B., Lee, M., Buell, A., Vu, B., Brgoch, J. & Willson, R. C. A low-cost smartphone-based platform for highly sensitive point-of-care testing with persistent luminescent phosphors. *Lab. Chip* **17**, 1051–1059 (2017).

52. Jacinto, M. J., Trabuco, J. R. C., Vu, B. V., Garvey, G., Khodadady, M., Azevedo, A. M., Aires-Barros, M. R., Chang, L., Kourentzi, K., Litvinov, D. & Willson, R. C. Enhancement of lateral flow assay performance by electromagnetic relocation of reporter particles. *PLOS ONE* **13**, e0186782 (2018).

53. Verma, H. N., Singh, P. & Chavan, R. M. Gold nanoparticle: synthesis and characterization. *Vet. World* **7**, 72–77 (2014).

54. Li, Z., Wang, Y., Wang, J., Tang, Z., Pounds, J. G. & Lin, Y. Rapid and Sensitive Detection of Protein Biomarker Using a Portable Fluorescence Biosensor Based on Quantum Dots and a Lateral Flow Test Strip. *Anal. Chem.* **82**, 7008–7014 (2010).

55. Niedbala, R. S., Feindt, H., Kardos, K., Vail, T., Burton, J., Bielska, B., Li, S., Milunic, D., Bourdelle, P. & Vallejo, R. Detection of Analytes by Immunoassay Using Up-Converting Phosphor Technology. *Anal. Biochem.* **293**, 22–30 (2001).

56. Härmä, H., Soukka, T. & Lövgren, T. Europium nanoparticles and time-resolved fluorescence for ultrasensitive detection of prostate-specific antigen. *Clin. Chem.* **47**, 561–568 (2001).

57. Paterson, A. S., Raja, B., Garvey, G., Kolhatkar, A., Hagström, A. E. V., Kourentzi, K., Lee, T. R. & Willson, R. C. Persistent Luminescence Strontium Aluminate Nanoparticles as Reporters in Lateral Flow Assays. *Anal. Chem.* **86**, 9481–9488 (2014).

58. Lateral Flow Immunoassay - Creative Diagnostics. Available at: https://www.creative-diagnostics.com/food-analysis/tag-lateral-flow-immunoassay-30.htm. (Accessed: 10th September 2019)

59. You, D. J., Park, T. S. & Yoon, J.-Y. Cell-phone-based measurement of TSH using Mie scatter optimized lateral flow assays. *Biosens. Bioelectron.* **40**, 180–185 (2013).

60. Gui, C., Wang, K., Li, C., Dai, X. & Cui, D. A CCD-based reader combined with CdS quantum dot-labeled lateral flow strips for ultrasensitive quantitative detection of CagA. *Nanoscale Res. Lett.* **9**, 57 (2014).

61. Cho, I.-H., Das, M., Bhandari, P. & Irudayaraj, J. High performance immunochromatographic assay combined with surface enhanced Raman spectroscopy. *Sens. Actuators B Chem.* **213**, 209–214 (2015).

62. Preechaburana, P., Suska, A. & Filippini, D. Biosensing with cell phones. *Trends Biotechnol.* **32**, 351–355 (2014).

63. Mudanyali, O., Dimitrov, S., Sikora, U., Padmanabhan, S., Navruz, I. & Ozcan, A. Integrated rapid-diagnostic-test reader platform on a cellphone. *Lab. Chip* **12**, 2678 (2012).

64. Lu, Y., Shi, W., Qin, J. & Lin, B. Low cost, portable detection of gold nanoparticle-labeled microfluidic immunoassay with camera cell phone. *ELECTROPHORESIS* **30**, 579–582 (2009).

65. Cho, S., Park, T. S., Nahapetian, T. G. & Yoon, J.-Y. Smartphone-based, sensitive µPAD detection of urinary tract infection and gonorrhea. *Biosens. Bioelectron.* **74**, 601–611 (2015).

66. Du, D., Wang, J., Wang, L., Lu, D. & Lin, Y. Integrated Lateral Flow Test Strip with Electrochemical Sensor for Quantification of Phosphorylated Cholinesterase: Biomarker of Exposure to Organophosphorus Agents. *Anal. Chem.* **84**, 1380–1385 (2012).

67. Qing, Y., Li, X., Chen, S., Zhou, X., Luo, M., Xu, X., Li, C. & Qiu, J. Differential pulse voltammetric ochratoxin A assay based on the use of an aptamer and hybridization chain reaction. *Microchim. Acta* **184**, 863–870 (2017).

68. Park, J.-M., Jung, H.-W., Chang, Y. W., Kim, H.-S., Kang, M.-J. & Pyun, J.-C. Chemiluminescence lateral flow immunoassay based on Pt nanoparticle with peroxidase activity. *Anal. Chim. Acta* **853**, 360–367 (2015).

69. van Dam, G. J., de Dood, C. J., Lewis, M., Deelder, A. M., van Lieshout, L., Tanke, H. J., van Rooyen, L. H. & Corstjens, P. L. A. M. A robust dry reagent lateral flow assay for diagnosis of active schistosomiasis by detection of Schistosoma circulating anodic antigen. *Exp. Parasitol.* **135**, 274–282 (2013).

70. Moghadam, B. Y., Connelly, K. T. & Posner, J. D. Two Orders of Magnitude Improvement in Detection Limit of Lateral Flow Assays Using Isotachophoresis. *Anal. Chem.* **87**, 1009–1017 (2015).

71. Adhikari, M., Strych, U., Kim, J., Goux, H., Dhamane, S., Poongavanam, M.-V., Hagström, A. E. V., Kourentzi, K., Conrad, J. C. & Willson, R. C. Aptamer-Phage Reporters for Ultrasensitive Lateral Flow Assays. *Anal. Chem.* **87**, 11660–11665 (2015).

72. Zhang, H., Xu, Y., Huang, Q., Yi, C., Xiao, T. & Li, Q. Natural phage nanoparticle-mediated real-time immuno-PCR for ultrasensitive detection of protein marker. *Chem. Commun.* **49**, 3778 (2013).

73. Chung, W.-J., Lee, D.-Y. & Yoo, S. Y. Chemical modulation of M13 bacteriophage and its functional opportunities for nanomedicine. *Int. J. Nanomedicine* **9**, 5825–5836 (2014).

74. Li, K., Chen, Y., Li, S., Nguyen, H. G., Niu, Z., You, S., Mello, C. M., Lu, X. & Wang, Q. Chemical Modification of M13 Bacteriophage and Its Application in Cancer Cell Imaging. *Bioconjug. Chem.* **21**, 1369–1377 (2010).

75. Mao, C. Virus-Based Toolkit for the Directed Synthesis of Magnetic and Semiconducting Nanowires. *Science* **303**, 213–217 (2004).

76. Urquhart, T., Daub, E. & Honek, J. F. Bioorthogonal Modification of the Major Sheath Protein of Bacteriophage M13: Extending the Versatility of Bionanomaterial Scaffolds. *Bioconjug. Chem.* **27**, 2276–2280 (2016).

77. Stopar, D., Spruijt, R. B., Wolfs, C. J. A. M. & Hemminga, M. A. Mimicking Initial Interactions of Bacteriophage M13 Coat Protein Disassembly in Model Membrane Systems. *Biochemistry* **37**, 10181–10187 (1998).

78. Clark, J. R. & March, J. B. Bacteriophages and biotechnology: vaccines, gene therapy and antibacterials. *Trends Biotechnol.* **24**, 212–218 (2006).

79. Clokie, M. R. J., Millard, A. D., Letarov, A. V. & Heaphy, S. Phages in nature. *Bacteriophage* **1**, 31–45 (2011).

80. Kim, J., Vu, B., Kourentzi, K., Willson, R. C. & Conrad, J. C. Increasing Binding Efficiency via Reporter Shape and Flux in a Viral Nanoparticle Lateral-Flow Assay. *ACS Appl. Mater. Interfaces* **9**, 6878–6884 (2017).

81. Citorik, R. J., Mimee, M. & Lu, T. K. Bacteriophage-based synthetic biology for the study of infectious diseases. *Curr. Opin. Microbiol.* **19**, 59–69 (2014).

82. Douglas, T. Viruses: Making Friends with Old Foes. *Science* **312**, 873–875 (2006).

83. Qian, S. & Bau, H. H. A mathematical model of lateral flow bioreactions applied to sandwich assays. *Anal. Biochem.* **322**, 89–98 (2003).

84. Gasperino, D., Baughman, T., Hsieh, H. V., Bell, D. & Weigl, B. H. Improving Lateral Flow Assay Performance Using Computational Modeling. *Annu. Rev. Anal. Chem.* **11**, 219–244 (2018).

85. Berli, C. L. A. & Kler, P. A. A quantitative model for lateral flow assays. *Microfluid. Nanofluidics* **20**, (2016).

86. Löfås, S., Malmqvist, M., Rönnberg, I., Stenberg, E., Liedberg, B. & Lundström, I. Bioanalysis with surface plasmon resonance. *Sens. Actuators B Chem.* **5**, 79–84 (1991).

87. Wartchow, C. A., Podlaski, F., Li, S., Rowan, K., Zhang, X., Mark, D. & Huang, K.-S. Biosensor-based small molecule fragment screening with biolayer interferometry. *J. Comput. Aided Mol. Des.* **25**, 669–676 (2011).

88. Xavier, K. A., Shick, K. A., Smith-Gil, S. J. & Willson, R. C. Involvement of water molecules in the association of monoclonal antibody HyHEL-5 with bobwhite quail lysozyme. *Biophys. J.* **73**, 2116–2125 (1997).

89. Kim, J., Poling-Skutvik, R., Trabuco, J. R. C., Kourentzi, K., Willson, R. C. & Conrad, J. C. Orientational binding modes of reporters in a viral-nanoparticle lateral flow assay. *The Analyst* **142**, 55–64 (2017).

90. Hosseini, S., Vázquez-Villegas, P. & Martínez-Chapa, S. O. Paper and Fiber-Based Bio-Diagnostic Platforms: Current Challenges and Future Needs. *Appl. Sci.* **7**, 863 (2017).

91. Chinnasamy, T., Segerink, L. I., Nystrand, M., Gantelius, J. & Andersson Svahn, H. Point-of-Care Vertical Flow Allergen Microarray Assay: Proof of Concept. *Clin. Chem.* **60**, 1209–1216 (2014).

92. Dupont, Y. A rapid-filtration technique for membrane fragments or immobilized enzymes: Measurements of substrate binding or ion fluxes with a few-millisecond time resolution. *Anal. Biochem.* **142**, 504–510 (1984).

93. Ligeti, E., Brandolin, G., Dupont, Y. & Vignais, P. V. Kinetics of Pi-Pi exchange in rat liver mitochondria. Rapid filtration experiments in the millisecond time range. *Biochemistry* **24**, 4423–4428 (1985).

94. Brandolin, G., Marty, I. & Vignais, P. V. Kinetics of nucleotide transport in rat heart mitochondria studied by a rapid filtration technique. *Biochemistry* **29**, 9720–9727 (1990).

95. Le Maire, M., Moeller, J. V. & Champeil, P. Binding of a nonionic detergent to membranes: flip-flop rate and location on the bilayer. *Biochemistry* **26**, 4803–4810 (1987).

96. Dupont, Y. & Moutin, M.-J. [62] Rapid filtration technique for metabolite fluxes across cell organelles. in *Methods in Enzymology* **148**, 675–683 (Elsevier, 1987).

97. Kim, H.-J., Rossotti, M. A., Ahn, K. C., González-Sapienza, G. G., Gee, S. J., Musker, R. & Hammock, B. D. Development of a noncompetitive phage anti-immunocomplex assay for brominated diphenyl ether 47. *Anal. Biochem.* **401**, 38–46 (2010).

98. Sambrook, J., Fritsch, E. & Maniatis, T. *Molecular cloning: A laboratory manual: Vol. 2*. (Cold Spring Harbor, 1989).

99. Branston, S., Stanley, E., Keshavarz-Moore, E. & Ward, J. Precipitation of filamentous bacteriophages for their selective recovery in primary purification. *Biotechnol. Prog.* **28**, 129–136 (2012).

100. Kim, J., Adhikari, M., Dhamane, S., Hagström, A. E. V., Kourentzi, K., Strych, U., Willson, R. C. & Conrad, J. C. Detection of Viruses By Counting Single

Fluorescent Genetically Biotinylated Reporter Immunophage Using a Lateral Flow Assay. *ACS Appl. Mater. Interfaces* **7**, 2891–2898 (2015).

101. Pack, M., Hu, H., Kim, D.-O., Yang, X. & Sun, Y. Colloidal Drop Deposition on Porous Substrates: Competition among Particle Motion, Evaporation, and Infiltration. *Langmuir* **31**, 7953–7961 (2015).
102. Dou, R. & Derby, B. Formation of Coffee Stains on Porous Surfaces. *Langmuir* **28**, 5331–5338 (2012).
103. Malitson, I. H. Interspecimen Comparison of the Refractive Index of Fused Silica*,†. *J. Opt. Soc. Am.* **55**, 1205 (1965).
104. Amarasiri Fernando, S. & Wilson, G. S. Studies of the 'hook' effect in the one-step sandwich immunoassay. *J. Immunol. Methods* **151**, 47–66 (1992).
105. Rodbard, D., Feldman, Y., Jaffe, M. L. & Miles, L. E. M. Kinetics of two-site immunoradiometric ('sandwich') assays—II. *Immunochemistry* **15**, 77–82 (1978).
106. Kim, D. S., Kim, Y. T., Hong, S. B., Kim, J., Huh, N. S., Lee, M.-K., Lee, S. J., Kim, B. I., Kim, I. S., Huh, Y. S. & Choi, B. G. Development of Lateral Flow Assay Based on Size-Controlled Gold Nanoparticles for Detection of Hepatitis B Surface Antigen. *Sensors* **16**, (2016).
107. Tang, R., Yang, H., Choi, J. R., Gong, Y., Hu, J., Feng, S., Pingguan-Murphy, B., Mei, Q. & Xu, F. Improved sensitivity of lateral flow assay using paper-based sample concentration technique. *Talanta* **152**, 269–276 (2016).

108. Cho, D. G., Yoo, H., Lee, H., Choi, Y. K., Lee, M., Ahn, D. J. & Hong, S. High-Speed Lateral Flow Strategy for a Fast Biosensing with an Improved Selectivity and Binding Affinity. *Sensors* **18**, (2018).

109. Tang, R., Yang, H., Gong, Y., Liu, Z., Li, X., Wen, T., Qu, Z., Zhang, S., Mei, Q. & Xu, F. Improved Analytical Sensitivity of Lateral Flow Assay using Sponge for HBV Nucleic Acid Detection. *Sci. Rep.* **7**, (2017).

110. Shi, C. Y., Deng, N., Liang, J. J., Zhou, K. N., Fu, Q. Q. & Tang, Y. A fluorescent polymer dots positive readout fluorescent quenching lateral flow sensor for ractopamine rapid detection. *Anal. Chim. Acta* **854**, 202–208 (2015).

111. Choi, D. H., Lee, S. K., Oh, Y. K., Bae, B. W., Lee, S. D., Kim, S., Shin, Y.-B. & Kim, M.-G. A dual gold nanoparticle conjugate-based lateral flow assay (LFA) method for the analysis of troponin I. *Biosens. Bioelectron.* **25**, 1999–2002 (2010).

112. Kim, H.-J., Ahn, K. C., González-Techera, A., González-Sapienza, G. G., Gee, S. J. & Hammock, B. D. Magnetic bead-based phage anti-immunocomplex assay (PHAIA) for the detection of the urinary biomarker 3-phenoxybenzoic acid to assess human exposure to pyrethroid insecticides. *Anal. Biochem.* **386**, 45–52 (2009).

113. Kim, H.-J., McCoy, M., Gee, S. J., González-Sapienza, G. G. & Hammock, B. D. Noncompetitive Phage Anti-Immunocomplex Real-Time Polymerase Chain Reaction for Sensitive Detection of Small Molecules. *Anal. Chem.* **83**, 246–253 (2011).

114. Sidhu, S. S. Engineering M13 for phage display. *Biomol. Eng.* **18**, 57–63 (2001).

115. Aubrey, K. L. & Thomas, G. J. Raman spectroscopy of filamentous bacteriophage Ff (fd, M13, f1) incorporating specifically-deuterated alanine and tryptophan side chains. Assignments and structural interpretation. *Biophys. J.* **60**, 1337–1349 (1991).

116. Bernard, J. M. L. & Francis, M. B. Chemical strategies for the covalent modification of filamentous phage. *Front. Microbiol.* **5**, (2014).

117. Domaille, D. W., Lee, J. H. & Cha, J. N. High density DNA loading on the M13 bacteriophage provides access to colorimetric and fluorescent protein microarray biosensors. *Chem. Commun.* **49**, 1759 (2013).

118. Li, H., Han, D., Pauletti, G. M. & Steckl, A. J. Blood coagulation screening using a paper-based microfluidic lateral flow device. *Lab Chip* **14**, 4035–4041 (2014).

119. Schneider, C. A., Rasband, W. S. & Eliceiri, K. W. NIH Image to ImageJ: 25 years of image analysis. *Nat. Methods* **9**, 671 (2012).

120. EMD Millipore. *Rapid Lateral Flow Test Strips: Considerations for Product Development*.

121. Huang, X., Aguilar, Z. P., Xu, H., Lai, W. & Xiong, Y. Membrane-based lateral flow immunochromatographic strip with nanoparticles as reporters for detection: A review. *Biosens. Bioelectron.* **75**, 166–180 (2016).

122. Borse, V. & Srivastava, R. Process parameter optimization for lateral flow immunosensing. *Mater. Sci. Energy Technol.* **2**, 434–441 (2019).

123. Market, F.-C. *The Immunoassay Handbook: Theory and applications of ligand binding, ELISA and related techniques*. (2013).

124. Roughton, B. C., Iyer, L. K., Bertelsen, E., Topp, E. M. & Camarda, K. V. Protein aggregation and lyophilization: Protein structural descriptors as predictors of aggregation propensity. *Comput. Chem. Eng.* **58**, 369–377 (2013).

125. Franks, F. Freeze-drying of bioproducts: putting principles into practice. *Eur. J. Pharm. Biopharm.* **45**, 221–229 (1998).

126. Jones, K. FUSION 5: A New Platform For Lateral Flow Immunoassay Tests. in *Lateral Flow Immunoassay* (eds. Wong, R. & Tse, H.) 1–15 (Humana Press, 2009). doi:10.1007/978-1-59745-240-3_7

127. Qiu, X., Thompson, J. A., Chen, Z., Liu, C., Chen, D., Ramprasad, S., Mauk, M. G., Ongagna, S., Barber, C., Abrams, W. R., Malamud, D., Corstjens, P. L. A. M. & Bau, H. H. Finger-actuated, self-contained immunoassay cassettes. *Biomed. Microdevices* **11**, 1175–1186 (2009).

128. Anfossi, L., Baggiani, C., Giovannoli, C., Biagioli, F., D'Arco, G. & Giraudi, G. Optimization of a lateral flow immunoassay for the ultrasensitive detection of aflatoxin M1 in milk. *Anal. Chim. Acta* **772**, 75–80 (2013).

129. Wang, J., Ahmad, H., Ma, C., Shi, Q., Vermesh, O., Vermesh, U. & Heath, J. A self-powered, one-step chip for rapid, quantitative and multiplexed detection of proteins from pinpricks of whole blood. *Lab. Chip* **10**, 3157 (2010).

130. Songjaroen, T., Dungchai, W., Chailapakul, O., Henry, C. S. & Laiwattanapaisal, W. Blood separation on microfluidic paper-based analytical devices. *Lab. Chip* **12**, 3392 (2012).

131. de la Escosura-Muñiz, A. & Merkoçi, A. A Nanochannel/Nanoparticle-Based Filtering and Sensing Platform for Direct Detection of a Cancer Biomarker in Blood. *Small* **7**, 675–682 (2011).

132. Brands, J., Kliner, D., Lipowsky, H. H., Kameneva, M. V., Villanueva, F. S. & Pacella, J. J. New insights into the microvascular mechanisms of drag reducing polymers: effect on the cell-free layer. *PloS One* **8**, e77252 (2013).

133. Choi, J. R., Hu, J., Feng, S., Wan Abas, W. A. B., Pingguan-Murphy, B. & Xu, F. Sensitive biomolecule detection in lateral flow assay with a portable temperature–humidity control device. *Biosens. Bioelectron.* **79**, 98–107 (2016).

134. Ciocca, D. R., Adams, D. J., Bjercke, R. J., Sledge, G. W., Edwards, D. P., Chamness, G. C. & McGuire, W. L. Monoclonal antibody storage conditions, and concentration effects on immunohistochemical specificity. *J. Histochem. Cytochem.* **31**, 691–696 (1983).

135. Cleland, J. L., Lam, X., Kendrick, B., Yang, J., Yang, T., Overcashier, D., Brooks, D., Hsu, C. & Carpenter, J. F. A specific molar ratio of stabilizer to protein is required for storage stability of a lyophilized monoclonal antibody. *J. Pharm. Sci.* **90**, 310–321 (2001).

136. Fischer, S., Hoernschemeyer, J. & Mahler, H. Glycation during storage and administration of monoclonal antibody formulations. *Eur. J. Pharm. Biopharm.* **70**, 42–50 (2008).

137. Yan, X., Huang, Z., He, M., Liao, X., Zhang, C., Yin, G. & Gu, J. Detection of HCG-antigen based on enhanced photoluminescence of hierarchical ZnO arrays. *Colloids Surf. B Biointerfaces* **89**, 86–92 (2012).

138. Goldstein, S. R., Snyder, J. R., Watson, C. & Danon, M. Very early pregnancy detection with endovaginal ultrasound. *Obstet. Gynecol.* **72**, 200–204 (1988).

139. Kosasa, T., Levesque, L., Goldstein, D. P. & Taymor, M. L. EARLY DETECTION OF IMPLANTATION USING A RADIOIMMUNOASSAY SPECIFIC FOR HUMAN CHORIONIC GONADOTROPIN. *J. Clin. Endocrinol. Metab.* **36**, 622–624 (1973).

140. Schneider, B. H., Dickinson, E. L., Vach, M. D., Hoijer, J. V. & Howard, L. V. Optical chip immunoassay for hCG in human whole blood. *Biosens. Bioelectron.* **15**, 597–604 (2000).

141. Ghosh, S. & Ahn, C. H. Lyophilization of chemiluminescent substrate reagents for high-sensitive microchannel-based lateral flow assay (MLFA) in point-of-care (POC) diagnostic system. *The Analyst* **144**, 2109–2119 (2019).

142. Ramachandran, S., Fu, E., Lutz, B. & Yager, P. Long-term dry storage of an enzyme-based reagent system for ELISA in point-of-care devices. *The Analyst* **139**, 1456–1462 (2014).

143. Mak, W. C., Beni, V. & Turner, A. P. F. Lateral-flow technology: From visual to instrumental. *TrAC Trends Anal. Chem.* **79**, 297–305 (2016).

144. Fu, E., Liang, T., Houghtaling, J., Ramachandran, S., Ramsey, S. A., Lutz, B. & Yager, P. Enhanced Sensitivity of Lateral Flow Tests Using a Two-Dimensional Paper Network Format. *Anal. Chem.* **83**, 7941–7946 (2011).

145. Parolo, C., Medina-Sánchez, M., de la Escosura-Muñiz, A. & Merkoçi, A. Simple paper architecture modifications lead to enhanced sensitivity in nanoparticle based lateral flow immunoassays. *Lab Chip* **13**, 386–390 (2013).

146. Shan, S., Lai, W., Xiong, Y., Wei, H. & Xu, H. Novel Strategies To Enhance Lateral Flow Immunoassay Sensitivity for Detecting Foodborne Pathogens. *J. Agric. Food Chem.* **63**, 745–753 (2015).

147. Peng, T., Yang, W., Lai, W.-H., Xiong, Y.-H., Wei, H. & Zhang, J. Improvement of the stability of immunochromatographic assay for the quantitative detection of clenbuterol in swine urine. *Anal Methods* **6**, 7394–7398 (2014).

148. Juntunen, E., Arppe, R., Kalliomäki, L., Salminen, T., Talha, S. M., Myyryläinen, T., Soukka, T. & Pettersson, K. Effects of blood sample anticoagulants on lateral flow assays using luminescent photon-upconverting and Eu(III) nanoparticle reporters. *Anal. Biochem.* **492**, 13–20 (2016).

149. Posthuma-Trumpie, G. A., Korf, J. & van Amerongen, A. Development of a competitive lateral flow immunoassay for progesterone: influence of coating conjugates and buffer components. *Anal. Bioanal. Chem.* **392**, 1215–1223 (2008).

150. Kovacs, E. W., Hooker, J. M., Romanini, D. W., Holder, P. G., Berry, K. E. & Francis, M. B. Dual-Surface-Modified Bacteriophage MS2 as an Ideal Scaffold for a Viral Capsid-Based Drug Delivery System. *Bioconjug. Chem.* **18**, 1140–1147 (2007).

151. Niu, Z., Bruckman, M. A., Harp, B., Mello, C. M. & Wang, Q. Bacteriophage M13 as a scaffold for preparing conductive polymeric composite fibers. *Nano Res.* **1**, 235–241 (2008).